

Composite Higgs Search at the LHC

J.R. Espinosa^{a,b}, C. Grojean^{b,c} and M. Mühlleitner^d

^a*ICREA, Institució Catalana de Recerca i Estudis Avançats, Barcelona, Spain*
at *IFAE, Universitat Autònoma de Barcelona, 08193 Bellaterra, Barcelona, Spain*

^b*CERN, Physics Department, Theory Unit, CH-1211 Geneva 23, Switzerland*

^c*Institut de Physique Théorique, CEA Saclay, F-91191 Gif-sur-Yvette, France*

^d*Institut für Theoretische Physik, Karlsruhe Institut of Technology, 76128 Karlsruhe, Germany*

Abstract

The Higgs boson production cross-sections and decay rates depend, within the Standard Model (SM), on a single unknown parameter, the Higgs mass. In composite Higgs models where the Higgs boson emerges as a pseudo-Goldstone boson from a strongly-interacting sector, additional parameters control the Higgs properties which then deviate from the SM ones. These deviations modify the LEP and Tevatron exclusion bounds and significantly affect the searches for the Higgs boson at the LHC. In some cases, all the Higgs couplings are reduced, which results in deterioration of the Higgs searches but the deviations of the Higgs couplings can also allow for an enhancement of the gluon-fusion production channel, leading to higher statistical significances. The search in the $H \rightarrow \gamma\gamma$ channel can also be substantially improved due to an enhancement of the branching fraction for the decay of the Higgs boson into a pair of photons.

1 Introduction

The massive nature of the weak gauge bosons requires new degrees of freedom and/or new dynamics around the TeV scale to act as an ultraviolet (UV) moderator and ensure a proper decoupling at high energy of the longitudinal polarizations W_L^\pm, Z_L . It is remarkable that a simple elementary weak-doublet not only provides the three Nambu–Goldstone bosons that will become the spin-1 longitudinal degrees of freedom but also contains an extra physical scalar field, the notorious Higgs boson, that screens the gauge-boson non-Abelian self-interaction contributions to scattering amplitudes and hence offers a consistent description of massive spin-1 particles. The minimality of this ElectroWeak Symmetry Breaking (EWSB) sector comes as a result of a highly constrained structure among the couplings of the Higgs doublet to the other Standard Model (SM) particles: a single parameter, the mass of the physical Higgs boson, dictates all the physical properties of the Higgs sector. Despite intensive searches over the last 20 years, no experimental results have been able to establish the reality of this theoretical paradigm. However, a harvest of electroweak precision data accumulated during these experimental searches, together with the absence of large flavor-changing neutral currents, suggests that violent departures from this minimal Higgs mechanism are unlikely, and rather call for smooth deformations, at least at low energy.

This provides a plausible motivation for considering a light Higgs boson emerging as a pseudo-Goldstone boson from a strongly-coupled sector, the so-called Strongly Interacting Light Higgs (SILH) scenario [1,2]¹. At low energy, the particle content is identical to the SM one: there exists a light and narrow Higgs-like scalar but this particle is a bound state from some strong dynamics [4,5] and a mass gap separates the Higgs boson from the other usual resonances of the strong sector as a result of the Goldstone nature of the Higgs. Nevertheless, the rates for Higgs production and decay differ significantly from those in the minimal Higgs incarnation. The aim of the present work is to look at how the searches for a Higgs boson are affected by the modifications of its couplings. Reference [6] already studied the modification induced by the strong dynamics to the gluon-fusion Higgs production and it was argued that it could have an impact on the Higgs searches². We extend this analysis and estimate the experimental sensitivities in the main LHC search channels studied by ATLAS and CMS.

In the attempt of providing a simple theoretical picture to parametrize the Higgs couplings in composite models, Ref. [1] constructed an effective Lagrangian involving higher dimensional operators for the low energy degrees of freedom and concluded that, as far as the LHC studies are concerned, the Higgs properties are essentially governed by its mass plus two new parameters. The effective SILH Lagrangian should be seen as an expansion in $\xi = (v/f)^2$ where $v = 1/\sqrt{\sqrt{2}G_F} \approx 246$ GeV and f is the typical scale of the Goldstone bosons of the strong sector. Therefore, it can be used to describe composite Higgs models in the vicinity of the SM limit, $\xi \rightarrow 0$. To reach the technicolor limit [8], $\xi \rightarrow 1$, a resummation of the full series in ξ is needed. Explicit models, built in five-dimensional (5D) warped space, provide concrete examples of such a resummation. In our analysis, we will rely on two 5D models that exhibit different behaviors of the Higgs couplings that, we hope, will be representative of the various composite Higgs models. In these explicit models,

¹SILH models have some similarities with models where the role of the Higgs is played by a composite dilaton resulting from the spontaneous breaking of scale invariance. See Refs. [3] for a recent discussion.

²See also Refs. [7] for an analysis of the gluon-fusion Higgs production in similar but different contexts.

the two extra parameters that generically control the couplings³ of a composite Higgs boson are related to each other and the deviations from the SM Higgs couplings are only controlled by the parameter $\xi = (v/f)^2$ which varies from 0 to 1⁴. In that sense, our analysis is an exploration of the parameter space of composite models along some special directions only. A complementary, but more general, analysis relying on the two parameters of the SILH Lagrangian is also possible, but it would be restricted to the range of validity of the $(v/f)^2$ expansion and would not allow to approach the technicolor limit. For these reasons, we did not pursue it further.

Composite Higgs models offer a continuous deformation of the SM Higgs paradigm. Another possible deformation consists in playing with the anomalous dimension of the Higgs field like in Higgsless models [10], gaugephobic models [11], unHiggs models [12] and conformal technicolor models [13], whose effective 4D descriptions might involve some non-local operators to take into account the non-canonical dimension of the Higgs boson (see Refs. [14] for reviews of models of new physics at the TeV scale).

It should be stressed that the couplings of the Higgs boson in the SILH scenario are not the most general ones that would be allowed by the general principles of quantum field theory and the local and global symmetries of the models considered: for instance, the important anomalous couplings will have the same Lorentz structure as the SM ones. In principle, some couplings with a different Lorentz structure could also be expected, but these ones would be generated only via the exchange of heavy resonances of the strong sector and not directly by the strong dynamics of the Goldstone bosons, therefore they would be parametrically suppressed, at least by a factor $(f/m_\rho)^2$ ($m_\rho > 2.5$ TeV is the typical mass scale of these resonances), and are irrelevant for our analysis. For similar reasons and due to the Goldstone nature of the Higgs, a direct coupling of the Higgs boson to two gluons or two photons will always induce sub-leading effects compared with the ones we are considering⁵.

Higgs anomalous couplings are not by themselves a direct probe of the strong sector at the origin of EWSB. For that, one would need to wait for the direct production of the heavy resonances of the strong sector or to rely on the processes with two Goldstones in the final state, as in the WW scattering or in the double Higgs production by boson fusion [2], where the composite nature of the Higgs boson would manifest itself by a residual growth of the amplitudes above the Higgs mass. Nevertheless, the relative importance of the various Higgs production and decay channels can bring first insights on the dynamics that controls the Higgs sector.

The paper is organized as follows: in Section 2, we give the general parametrization of the couplings of a composite Higgs as derived from the SILH Lagrangian of Ref. [1] and, for the two explicit 5D composite Higgs models we will consider, we give the exact form of these couplings

³We will qualify these couplings as *anomalous* couplings since they differ from the SM ones.

⁴Similar deviations of the Higgs couplings are also present in extra-dimensional models where the Higgs mixes with the *radion* field [9], however, in that case, the deviations do not originate from strong interactions.

⁵ This statement will change when the SM fermions, and in particular the top quark, have a direct coupling to the strong sector. Then some top-partners are expected to give sizeable corrections to the $H\gamma\gamma$ and Hgg vertices (we will explore this possibility in a future work). On the contrary, when the fermions are elementary, all these corrections can be recast into a correction to the Yukawa couplings only and the $H\gamma\gamma$ and Hgg loop-induced vertices do not depend on the details of the resonance spectrum, hence, as announced, the Higgs physical properties do depend only on two extra parameters in addition to its mass. This structure is specific to SILH models and does not hold in general: indeed totally model-independent operator analyses [15,16] lead to the conclusion that the dominant effects should appear in the vertices $H\gamma\gamma$ and Hgg .

valid for values of ξ interpolating between the SM and the technicolor limits. The deviations in the Higgs decay rates are presented and the bounds on the Higgs mass at LEP and Tevatron are studied (Section 3). Section 4 contains our main results: we first discuss the modifications, due to the composite nature of the Higgs boson, of the Higgs production cross-sections including the next-to-leading order QCD corrections and then we re-examine the various search channels for a Higgs boson at the LHC computing the changes in their statistical significance. At low values of ξ , the searches are made more difficult due to a general reduction of all the Higgs couplings, but for larger values of ξ , it is possible to increase the significance thanks, in particular, to an enhanced Higgs production by gluon fusion, though this enhancement is model-dependent. Finally, in Section 5, we combine the various search channels and we present our conclusions. In the appendix, we collect the various estimators of the statistical significance we use in our analysis.

2 General parametrization of the Higgs couplings

2.1 SILH couplings

The effective Lagrangian describing a SILH involves higher dimensional operators. There are two classes of higher dimensional operators: (i) those that are genuinely sensitive to the new strong force and will affect qualitatively the physics of the Higgs boson and (ii) those that are sensitive to the spectrum of the resonances only and will simply act as form factors. Simple rules control the size of these different operators (see Ref. [1]) and the effective Lagrangian generically takes the form

$$\begin{aligned} \mathcal{L}_{\text{SILH}} = & \frac{c_H}{2f^2} (\partial_\mu |H|^2)^2 + \frac{c_T}{2f^2} \left(H^\dagger \overleftrightarrow{D}_\mu H \right)^2 - \frac{c_6 \lambda}{f^2} |H|^6 + \left(\frac{c_y y_f}{f^2} |H|^2 \bar{f}_L H f_R + \text{h.c.} \right) \\ & + \frac{ic_W g}{2m_\rho^2} \left(H^\dagger \sigma^i \overleftrightarrow{D}^\mu H \right) (D^\nu W_{\mu\nu})^i + \frac{ic_B g'}{2m_\rho^2} \left(H^\dagger \overleftrightarrow{D}^\mu H \right) (\partial^\nu B_{\mu\nu}) + \dots \end{aligned} \quad (1)$$

where g, g' are the SM EW gauge couplings, λ is the SM Higgs quartic coupling and y_f is the SM Yukawa coupling to the fermions $f_{L,R}$. All the coefficients, $c_H, c_T \dots$, appearing in Eq. (1) are expected to be of order one unless protected by some symmetry. For instance, in every model in which the strong sector preserves custodial symmetry, the coefficient c_T vanishes and only three coefficients, c_H, c_y and c_6 , give sizable contributions to the Higgs (self-)couplings. The operator c_H gives a correction to the Higgs kinetic term which can be brought back to its canonical form at the price of a proper rescaling of the Higgs field, inducing a universal shift of the Higgs couplings by a factor $1 - c_H \xi/2$. For the fermions, this universal shift adds up to the modification of the Yukawa interactions

$$g_{Hf\bar{f}}^\xi = g_{Hf\bar{f}}^{\text{SM}} \times [1 - (c_y + c_H/2)\xi], \quad (2)$$

$$g_{HVV}^\xi = g_{HVV}^{\text{SM}} \times (1 - c_H \xi/2), \quad g_{HHVV}^\xi = g_{HHVV}^{\text{SM}} \times (1 - 2c_H \xi) \quad (3)$$

where $V = W, Z$, $g_{Hf\bar{f}}^{\text{SM}} = m_f/v$ (m_f denotes the fermion mass), $g_{HW+W-}^{\text{SM}} = gM_W$, $g_{HZZ}^{\text{SM}} = \sqrt{g^2 + g'^2} M_Z$, $g_{HHW+W-}^{\text{SM}} = g^2/2$ and $g_{HHZZ}^{\text{SM}} = (g^2 + g'^2)/2$. As announced in the Introduction, all the dominant corrections, i.e., the ones controlled by the strong operators, preserve the Lorentz structure of the SM interactions, while the form factor operators will also introduce couplings with a different Lorentz structure.

2.2 Higgs anomalous couplings in two concrete models

The Holographic Higgs models of Refs. [17–19] are based on a five-dimensional theory in Anti de-Sitter (AdS) space-time. The bulk gauge symmetry $SO(5) \times U(1)_X \times SU(3)$ is broken down to the SM gauge group on the UV boundary and to $SO(4) \times U(1)_X \times SU(3)$ on the IR. Since the symmetry-breaking pattern of the bulk and IR boundary is given by $SO(5) \rightarrow SO(4)$, we expect four Goldstone bosons parametrized by the $SO(5)/SO(4)$ coset [18]:

$$\Sigma = \langle \Sigma \rangle e^{\Pi/f}, \quad \langle \Sigma \rangle = (0, 0, 0, 0, 1), \quad \Pi = \begin{pmatrix} 0_4 & \mathcal{H} \\ -\mathcal{H}^T & 0 \end{pmatrix}, \quad (4)$$

where \mathcal{H} is a real 4-component vector, which transforms as a doublet under the weak $SU(2)$ group and can be associated with the Higgs. The couplings between the Higgs boson and the gauge fields are obtained from the pion kinetic term

$$\mathcal{L}_{\text{kin}} = \frac{f^2}{2} (D_\mu \Sigma) (D^\mu \Sigma)^T. \quad (5)$$

In the unitary gauge where $\Sigma = (\sin H/f, 0, 0, 0, \cos H/f)$, Eq. (5) gives

$$\mathcal{L}_{\text{Kin}} = \frac{1}{2} \partial_\mu H \partial^\mu H + m_W^2(H) \left[W_\mu W^\mu + \frac{1}{2 \cos^2 \theta_W} Z_\mu Z^\mu \right] \quad \text{with} \quad m_W(H) = \frac{gf}{2} \sin \frac{H}{f}. \quad (6)$$

Expanding Eq. (6) in powers of the Higgs field, we obtain the Higgs couplings to the gauge fields

$$g_{HVV} = g_{HVV}^{\text{SM}} \sqrt{1 - \xi}, \quad g_{HHVV} = g_{HHVV}^{\text{SM}} (1 - 2\xi), \quad (7)$$

with the compositeness parameter ξ defined as

$$\xi = \left(\frac{v}{f} \right)^2 = \sin^2 \frac{\langle H \rangle}{f}. \quad (8)$$

The couplings of the Higgs boson to the fermions can be obtained in the same way, but they will depend on the way the SM fermions are embedded into representations of the bulk symmetry. In the MCHM4 model [18] with SM fermions transforming as spinorial representations of $SO(5)$, the interactions of the Higgs to the fermions take the form

$$\mathcal{L}_{\text{Yuk}} = -m_f(H) \bar{f} f \quad \text{with} \quad m_f(H) = M \sin \frac{H}{f}. \quad (9)$$

We then obtain

$$\text{MCHM4:} \quad g_{Hff} = g_{Hff}^{\text{SM}} \sqrt{1 - \xi}. \quad (10)$$

In the MCHM5 model [19] with SM fermions transforming as fundamental representations of $SO(5)$, the interactions of the Higgs to the fermions take the following form (M is a constant of mass-dimension one)

$$\mathcal{L}_{\text{Yuk}} = -m_f(H) \bar{f} f \quad \text{with} \quad m_f(H) = M \sin \frac{2H}{f}. \quad (11)$$

We then obtain

$$\text{MCHM5:} \quad g_{Hff} = g_{Hff}^{\text{SM}} \frac{1 - 2\xi}{\sqrt{1 - \xi}}. \quad (12)$$

In both models, the Higgs couplings to gauge boson are always reduced compared to the SM ones, as expected from the positivity theorem [20] on the c_H coefficient of the SILH Lagrangian. On the contrary, the two models exhibit different characteristic behaviors in the Higgs couplings to fermions: in the vicinity of the SM, i.e., for low values of ξ , the couplings are reduced, and the reduction is more important for MCHM5 than for MCHM4, but, for larger values of ξ , the couplings in MCHM5 are raising back and can even get much larger than the SM ones. This latter effect is at the origin of an enhancement of the Higgs production cross-section by gluon fusion, enhancement that will significantly affect the Higgs searches.

In the previous expressions for the anomalous Higgs couplings we keep the full ξ -dependence, without expanding in small ξ . In general, higher-order derivative operators for Σ would induce momentum dependent corrections to these couplings but, as discussed in Ref. [1], such contributions will be suppressed by powers of p^2/m_ρ^2 , and we neglect such effects.

2.3 Branching ratios and total widths

The partial widths in the composite Higgs models can be easily obtained from the SM partial widths by rescaling the couplings involved in the Higgs decays. Since in MCHM4 all Higgs couplings are modified by the same universal factor $\sqrt{1-\xi}$, the branching ratios are the same as in the SM model. The total width will be different though by an overall factor $1-\xi$.

In MCHM5, all partial widths for decays into fermions are obtained from the SM widths by multiplication with the modification factor of the Higgs Yukawa coupling squared,

$$\Gamma(H \rightarrow f\bar{f}) = \frac{(1-2\xi)^2}{(1-\xi)} \Gamma^{SM}(H \rightarrow f\bar{f}) . \quad (13)$$

The Higgs decay into gluons is mediated by heavy quark loops, so that the multiplication factor is the same as for the fermion decays:

$$\Gamma(H \rightarrow gg) = \frac{(1-2\xi)^2}{(1-\xi)} \Gamma^{SM}(H \rightarrow gg) . \quad (14)$$

For the Higgs decays to massive gauge bosons V we obtain

$$\Gamma(H \rightarrow VV) = (1-\xi) \Gamma^{SM}(H \rightarrow VV) . \quad (15)$$

The Higgs decay into photons proceeds dominantly via W -boson and top and bottom loops. Since the couplings to gauge bosons and fermions scale differently in MCHM5, the various loop contributions have to be multiplied with the corresponding Higgs coupling modification factor. The leading order width is given by

$$\Gamma(H \rightarrow \gamma\gamma) = \frac{\Gamma^{SM}(H \rightarrow \gamma\gamma)}{[I_\gamma(M_H) + J_\gamma(M_H)]^2} \left[\frac{1-2\xi}{\sqrt{1-\xi}} I_\gamma(M_H) + \sqrt{1-\xi} J_\gamma(M_H) \right]^2 , \quad (16)$$

where

$$\begin{aligned} I_\gamma(M_H) &= \frac{4}{3} F_{1/2}(4M_t^2/M_H^2), \quad J_\gamma(M_H) = F_1(4M_W^2/M_H^2), \\ F_{1/2}(x) &\equiv -2x[1 + (1-x)f(x)], \quad F_1(x) \equiv 2 + 3x[1 + (2-x)f(x)], \\ f(x) &\equiv \arcsin[1/\sqrt{x}]^2 \text{ for } x \geq 1 \text{ and } f(x) \equiv -\frac{1}{4} \left[\log \frac{1+\sqrt{1-x}}{1-\sqrt{1-x}} - i\pi \right]^2 \text{ for } x < 1. \end{aligned} \quad (17)$$

Both decays into gluons and photons are loop-induced and might in principle be affected by possible new particles running in the loops. The set-ups we are considering, however, assume that the only chiral degrees of freedom the Higgs couples to are the SM ones (see footnote 5). This will certainly be modified if the top quark, for instance, is a composite particle since additional top-partners would then also be expected to have a significant coupling to the Higgs (see for instance Ref. [21]). Under our original assumption, the corrections to the $H\gamma\gamma$ and Hgg vertices originate from the modified Yukawa interactions only and the loop-decays can be safely computed in the framework of our effective theory. The higher order corrections to the decays are unaffected as long as QCD corrections are concerned, since they do not involve the Higgs couplings.

We have calculated the Higgs branching ratios with the program HDECAY [22] where we have implemented the modifications due to the composite model described above. The program HDECAY includes the most important higher order corrections to the various Higgs decays and includes the off-shell effects in the Higgs decays into massive gauge bosons and a top quark pair.

Figure 1 shows the branching ratios in the SM and those of MCHM5 for three representative values of $\xi = 0.2, 0.5, 0.8$. The Higgs mass range has been chosen between 80 and 200 GeV, which is the mass range favoured by composite Higgs models. Notice that the lower mass range has not been excluded yet completely by the LEP bounds (see Section 3).

The SM branching ratios show the typical behaviour dictated by the Higgs mechanism, which predicts the Higgs couplings to the matter particles to be proportional to the mass of these particles. A Higgs boson in the intermediate mass range, $\mathcal{O}(M_Z) \leq M_H \leq \mathcal{O}(2M_Z)$, dominantly decays into a $b\bar{b}$ pair and a pair of massive gauge bosons, one or two of them being virtual. Above the gauge boson threshold, it almost exclusively decays into WW, ZZ , with a small admixture of top decays near the $t\bar{t}$ threshold (not visible in this Figure, being outside the mass range plotted here). Below ~ 140 GeV the decays into $\tau^+\tau^-$, $c\bar{c}$ and gg are important besides the dominant $b\bar{b}$ decay. The $\gamma\gamma$ decay, though very small, provides a clear 2-body signature for the Higgs production in this mass range. The branching ratios in MCHM4 are exactly the same as in the SM, since all couplings scale with the same modification factor, which then drops out in the branching ratios.

As can be inferred from Figs. 1, for non-vanishing ξ values, the branching ratios (BRs) in MCHM5 can change considerably. The behaviour can be easily understood by looking at Fig. 2 which shows the same branching ratios as a function of ξ for two representative values of the Higgs boson mass, $M_H = 120$ GeV and 180 GeV. The BRs into fermions are governed by the $(1 - 2\xi)^2/(1 - \xi)$ prefactor of the corresponding partial widths: as ξ increases from 0, there is first a decrease of the fermionic BRs, until they vanish at $\xi = 0.5$ and then grow again with larger ξ . The same behaviour is observed in the decay into gluons, which is loop-mediated by quarks. The decays into gauge bosons show a complementary behaviour: for small ξ , due to the decreasing decay widths into fermions, the importance of the vector boson decays becomes more and more pronounced until a maximum value at $\xi = 0.5$ is reached. Above this value the branching ratios into gauge boson decrease with increasing Higgs decay widths into fermion final states: the Higgs boson becomes gaugephobic in the technicolor limit ($\xi \rightarrow 1$).

Coming back to Fig. 1, we see that for small $\xi = 0.2$, the decays into massive and massless gauge bosons set in at lower Higgs mass values and are more important than in the SM. The BR into $\gamma\gamma$, especially important for low Higgs mass searches at the LHC, is larger now. The branching ratio

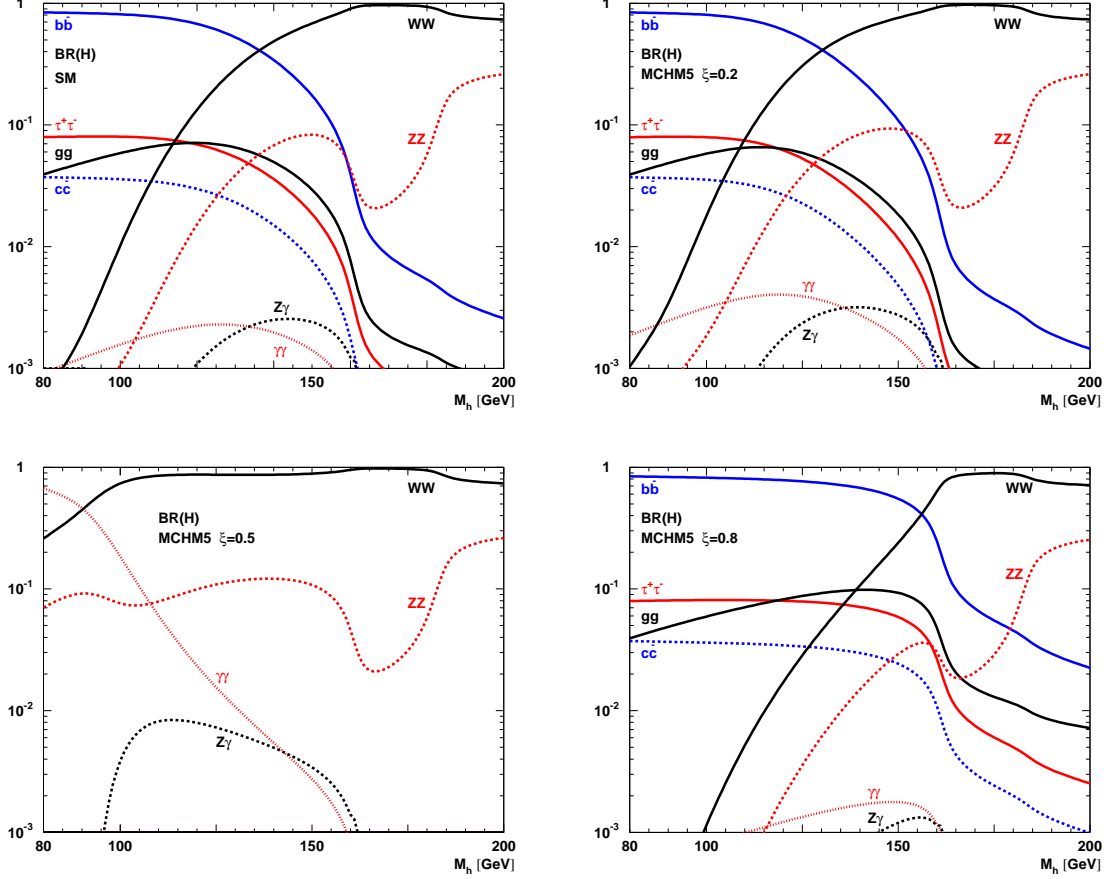


Figure 1: Higgs branching ratios as a function of the Higgs boson mass in the SM ($\xi = 0$, upper left) and MCHM5 with $\xi = 0.2$ (upper right), 0.5 (bottom left) and 0.8 (bottom right).

into $b\bar{b}$ gets less important, an effect that is more visible at higher Higgs masses. This behaviour culminates at $\xi = 0.5$, where only decays into gauge bosons are present due to the closure of the decays into fermions⁶. In particular, the Higgs decay mode into photons can reach large values up to $\sim 70\%$ at 80 GeV in this case. Note also that, for $\xi = 0.5$, the decay into a pair of gluons is also absent since the Higgs does not couple to the top quark. In practice, however, such a decay can be mediated by the heavy vector resonances of the strong sector. Also the branching ratios into massive gauge bosons are significant at low Higgs masses, while above the gauge boson thresholds they approach their SM values. For large $\xi = 0.8$, the low Higgs mass region is dominated by the decays into heavy fermions. The branching ratios extend to somewhat higher Higgs mass values

⁶ Instead the Higgs boson could decay into fermions through an electroweak particle-loop (note that the interference term with the tree-level decay is absent since the tree-level amplitude is vanishing) and the decay could in principle compete with the $\gamma\gamma$ decay, which is also loop mediated and plays an important role for small Higgs masses. However, in addition to the loop suppression, the decay into light fermions has an additional suppression factor of order m_f^2/M^2 where m_f is the light fermion mass and M is a mass of electroweak size that can be either the Higgs mass, the top mass or the W mass depending on the diagram involved. We have checked numerically that this loop decay channel into $b\bar{b}$ is about 2 orders of magnitude subdominant compared to the $\gamma\gamma$ decay. Similarly, a fermiophobic Higgs boson can also decay radiatively into two gluons, but this 2-loop EW process will be totally negligible.

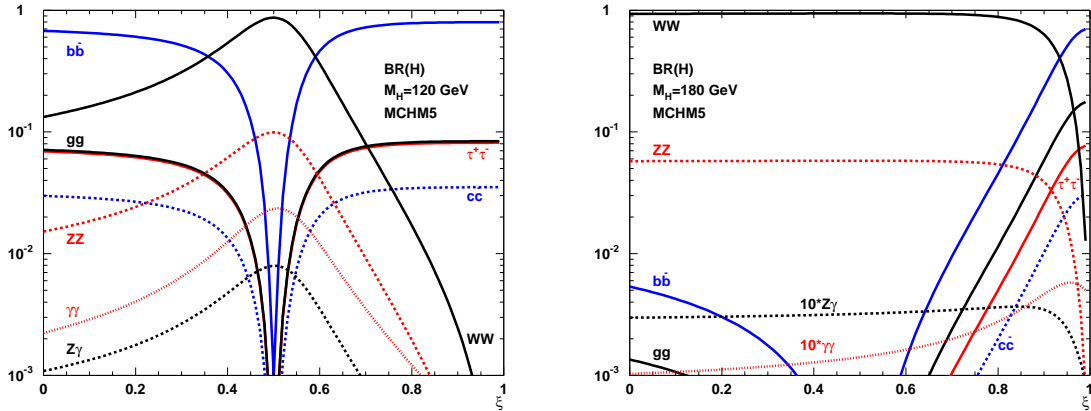


Figure 2: The branching ratios of MCHM5 as a function of ξ for $M_H = 120$ GeV (left) and $M_H = 180$ GeV (right).

than in the SM. The onset of the gauge boson decays is postponed to Higgs mass values larger than in the SM.

Figure 3 shows the Higgs width as a function of M_H in the SM and for $\xi = 0.2, 0.5$ and 0.8 both in MCHM4 (left plot) and MCHM5 (right plot). Below ~ 150 GeV, the width is rather small and increases rapidly as the vector boson decay channels open up. The Higgs width in MCHM4 and MCHM5 is also plotted in Fig. 4 in the (M_H, ξ) plane. In MCHM4, the total width decreases monotonously with rising ξ due to the rescaling of the couplings with $\sqrt{1-\xi}$. In MCHM5, the total width develops a pronounced minimum at $\xi = 0.5$ for low Higgs mass values (the light region on the right plot of Fig. 4). The origin of this minimum is of course the reduced couplings to fermions which even vanish identically at $\xi = 0.5$. For larger values of ξ , the fermionic channels reopen and the total width rises with growing ξ . At large Higgs masses the total width is dominated by gauge boson decays at low ξ values, since we are above the gauge boson threshold here. At large ξ values the role is taken over by the fermion decays, which do not become as large as the gauge boson decays, however, so that also in the limit $\xi \rightarrow 1$, for large Higgs mass values the total width remains below the SM value at $\xi = 0$. A small total width may be of advantage for Higgs boson searches since more stringent mass cuts could be applied in that case. However, in our analysis, we will simply study how the Higgs searches rescale with ξ and we will not try to optimize the cuts used in the SM searches to a different Higgs width.

3 Constraints from LEP, the Tevatron and electroweak precision data

Higgs searches at LEP and the Tevatron set constraints on the parameter space (M_H, ξ) of the composite Higgs models we consider. Figure 5 shows the excluded regions for MCHM4 (left) and MCHM5 (right). To generate the plots we have used the Higgsbounds program [23], cross-checking the results wherever possible and modifying it suitably to take into account the latest changes in Tevatron limits.

At LEP, the most relevant search channel is $e^+e^- \rightarrow ZH \rightarrow Zb\bar{b}$ [24], which is sensitive both to the Higgs-gauge coupling (in Higgs-strahlung production) and to the Higgs-fermion coupling (in

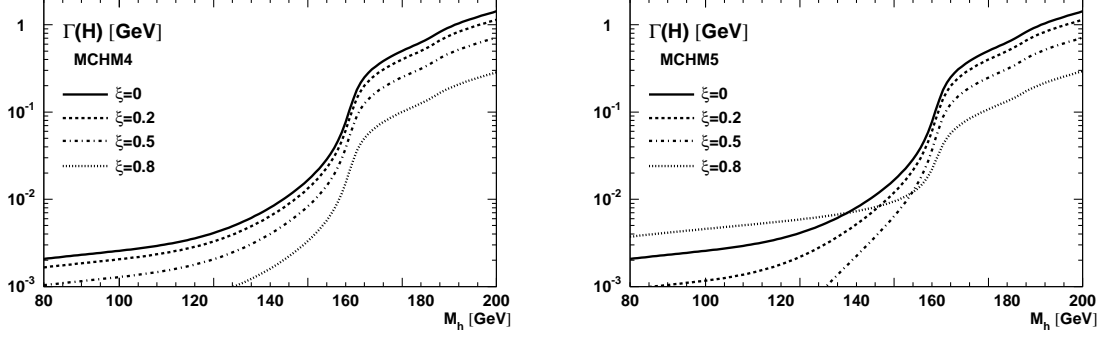


Figure 3: The Higgs total width Γ_H (in GeV) vs. M_H (in GeV) in the SM (continuous line) and for $\xi = 0.2$ (dashed), $\xi = 0.5$ (dot-dashed) and $\xi = 0.8$ (dotted) in MCHM4 (left) and MCHM5 (right).

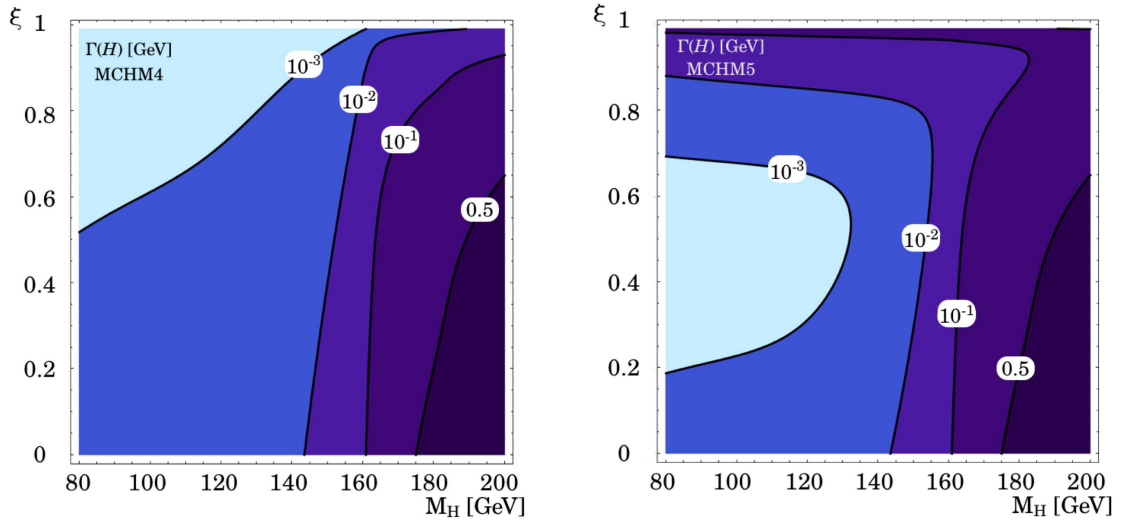


Figure 4: Contour plots of the Higgs total width, Γ_H , in the plane (M_H, ξ) for MCHM4 (left) and MCHM5 (right). The contours correspond to $\Gamma_H = 10^{-3}, 10^{-2}, 10^{-1}$ and 0.5 GeV.

the Higgs decay). The former coupling is reduced in both models and explains why the SM lower Higgs mass limit $M_H > 114.4$ GeV is degraded in the composite models, as shown in Figs. 5. In MCHM5, the Higgs-fermion coupling vanishes at $\xi = 0.5$ implying that the limit from the above process is lost in the neighbourhood of this ξ value. In this region the process $e^+e^- \rightarrow ZH \rightarrow Z\gamma\gamma$ can be exploited [25]. LEP sets a limit on $(\sigma_{ZH}/\sigma_{ZH}^{SM}) \times BR(H \rightarrow \gamma\gamma)$ which does not translate into a limit on M_H in the SM but is useful in our composite model to cover the $\xi = 0.5$ hole in the $H \rightarrow b\bar{b}$ LEP limit (see Fig. 5, right).

At the Tevatron, the most relevant search is through the $H \rightarrow WW$ decay, which in the SM excludes at 95% C.L. the mass range $162 \text{ GeV} < M_H < 166 \text{ GeV}$ [26]. In our composite models this excluded band shrinks to zero quickly once ξ slightly exceeds zero, as then the production cross-section (dominated by the gluon-fusion process) is reduced. In MCHM5, however, Tevatron can exclude a region with $M_H \sim 165 - 185$ GeV and large $\xi > 0.8$ through the channel $H \rightarrow WW$ with the W 's decaying leptonically [26]. This occurs thanks to the enhancement of Yukawa couplings

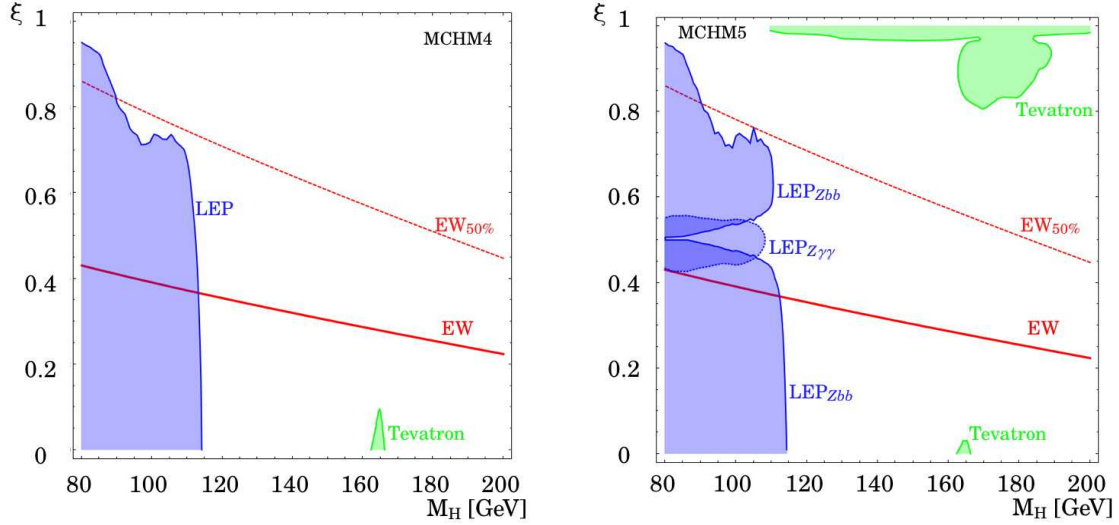


Figure 5: Experimental limits from Higgs searches at LEP (blue/dark gray) and the Tevatron (green/light gray) in the plane (M_H, ξ) for MCHM4 (left) and MCHM5 (right). EW precision data prefer low value of ξ : the red continuous line delineates the region favored at 99% CL (with a cutoff scale fixed at 2.5 TeV) while the region below the red dashed line survives if there is an additional 50% cancellation of the oblique parameters.

at large ξ , which boosts the gluon-fusion production mechanism while the WW branching ratio is still high (unless one is really close to $\xi = 1$, when fermionic decays take over). For such large values of ξ ($\xi \gtrsim 0.97$) in MCHM5, the decay $H \rightarrow \tau\tau$ would lead to an observable signature at the Tevatron [27] and the corresponding parameter region is also excluded (see Fig. 5, right). Nevertheless, this region is already at the border of the regime of nonperturbative Yukawa couplings (see below) where the validity of our computations is not guaranteed. In any case, these Tevatron exclusion bounds should be regarded as rough estimates. Indeed, the Tevatron collaborations combine different search channels in a very sophisticated way. The relative importance of the search channels in our concrete models changes, however, with varying ξ . For each ξ value, the search channels would have to be combined at the same level of sophistication as done by Tevatron analyses. This is clearly beyond the scope of our work, though. Nevertheless, the bounds presented in Fig 5 serve to get an approximate picture of exclusion regions due to Tevatron searches.

In the SM, the Higgs mass is notoriously constrained not only by direct searches but also by EW precision data. As is well known [28], the oblique parameters are indeed logarithmically sensitive to the Higgs mass. In composite models, there are three main contributions to the oblique parameters whose origin can be easily understood using the SILH effective Lagrangian (1): (i) The operator c_T gives a contribution to the T parameter, $\hat{T} = c_T v^2 / f^2$, which would impose a very large compositeness scale; however, assuming that the custodial symmetry is preserved by the strong sector, the coefficient of this operator is vanishing automatically. The explicit models we are considering fulfill this requirement. (ii) A contribution to the S parameter is generated by the form factor operators only, $\hat{S} = (c_W + c_B) M_W^2 / M_\rho^2$, and will simply impose a lower bound on the mass of the heavy resonances, $m_\rho \geq 2.5$ TeV. Throughout this paper, we have assumed that the mass gap between the Higgs boson and the other resonances of the strong sector is large enough to satisfy

this bound. (iii) Finally, there is a third contribution to the oblique parameters that will constrain the parameter space of our set-up: since the couplings of the Higgs to the SM vectors receive some corrections of the order ξ , the nice cancelation occurring in the SM between the Higgs and the gauge boson contributions to S and T does not hold anymore and they are both logarithmically divergent [29] (the divergence in T will eventually be screened by resonance states if the strong sector is invariant under the custodial symmetry). S and T , or equivalently $\epsilon_{1,3}$ [30], can be easily estimated from the SM $\log(M_H)$ pieces

$$\begin{aligned} \text{SM: } \begin{cases} \delta\epsilon_1 \approx 8.6 \cdot 10^{-4} \times \log(M_H/M_Z) \\ \delta\epsilon_3 \approx 5.4 \cdot 10^{-4} \times \log(M_H/M_Z) \end{cases} \\ \Rightarrow \text{SILH: } \begin{cases} \delta\epsilon_1 \approx 8.6 \cdot 10^{-4} \times [\log(M_H/M_Z) - \xi \log(M_H/\Lambda)] \\ \delta\epsilon_3 \approx 5.4 \cdot 10^{-4} \times [\log(M_H/M_Z) - \xi \log(M_H/\Lambda)] \end{cases} \quad (18) \end{aligned}$$

Therefore, EW precision data prefer low values of the compositeness parameter ξ . In Fig. 5, we have plotted the upper bound on ξ as a function of the Higgs mass (continuous red line) obtained from the 99% CL limits on $\epsilon_{1,3}$. Allowing a partial cancellation of the order of 50% with contributions from other states, the upper bound on ξ is relaxed by a factor of about 2 (dashed red line).

Finally, it should also be mentioned that the limit $\xi \rightarrow 1$ is not fully consistent with basic perturbative requirements, in particular for MCHM5. Indeed, in deriving the Yukawa coupling of the top, we fixed the top mass to its experimental value, which requires some 5D coupling to become very large in the limit $\xi \rightarrow 1$. The exact perturbative limit depends on the details of the models and the way the top mass is actually generated. A simple estimate can be inferred by writing Eq. (11) with $M = \lambda f$ where λ is a dimensionless coupling that should be bounded from above. We will simply require $\lambda < 4\pi$, which gives

$$\xi < 1 - (m_t/(8\pi v))^2 \approx 0.999. \quad (19)$$

This limit, though certainly not very accurate, gives an idea on the maximal possible value for ξ .

4 LHC Searches

In the composite Higgs models, the Higgs boson search channels can be significantly changed compared to the SM case, due to the modified production cross-sections and branching ratios. As an extreme example, in MCHM5, the Higgs couplings to fermions will be absent for $\xi = 0.5$. In this case, the Higgs boson production through gluon fusion, which is dominant in the SM, cannot be exploited⁷. On the other hand the branching ratios into gauge bosons will be enhanced due to the absence of the decay into $b\bar{b}$ final states. In order to identify which search channels become important and which search strategy should be applied, we produced contour plots (in the (M_H, ξ) parameter plane) of the expected significances for different search channels in the two composite Higgs models discussed above. Before we present our results, we will first discuss how the production cross-sections of a composite Higgs boson change.

⁷In principle, when the Higgs boson decouples from the fermions, the gluon-fusion production process can still receive a contribution from the heavy resonances of the strong sector, but this contribution is negligible when the masses of these resonances are above 2–3 TeV as required by EW precision data. The 2-loop EW gluon-fusion process is also totally negligible.

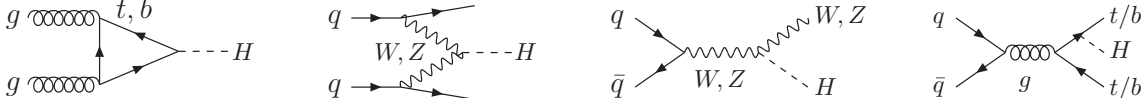


Figure 6: Generic diagrams contributing to Higgs production in gluon fusion, weak-boson fusion, Higgsstrahlung and associated production with heavy quarks.

4.1 Higgs boson production cross-sections

At the LHC, the relevant Higgs production processes (depicted in Fig. 6) are (for reviews, see Refs. [31,32])

Gluon fusion The gluon-fusion process $gg \rightarrow H$ [33] constitutes the most important Higgs production cross-section in the SM. At leading order, it is mediated by top and bottom quark loops. The next-to-leading order (NLO) QCD corrections have been obtained including the full mass dependence of the loop particles [34] as well as in the heavy top quark limit [34,35]. The NLO corrections increase the total cross-section by 50-100 %. The next-to-next-to leading order (NNLO) corrections have been determined in the heavy top quark limit enhancing the total cross-section by another 20% [36]. These results have been improved by soft-gluon resummation at next-to-next-to-leading log (NNLL) accuracy adding another $\sim 10\%$ to the total cross-section [37]. Recently, the top quark mass effects on the NNLO loop corrections have been investigated [38] and confirmed the heavy top limit as a reliable approximation in the small and intermediate Higgs mass range. Furthermore, the electroweak (EW) corrections have been evaluated and turned out to be small [39].

We have calculated the gluon-fusion cross-section including the NLO QCD corrections with the full mass dependence of the loop particles. This corresponds to the approximation used in the CMS analyses. Since the gluon-fusion cross-section is mediated by heavy quark loops and the NLO QCD corrections do not affect the Higgs couplings, the gluon-fusion composite-Higgs production cross-section is obtained from the NLO QCD SM cross-section by the squared rescaling factor for the Higgs Yukawa coupling [see Eqs. (10) and (12)], hence⁸

$$\begin{aligned} \sigma_{NLO}(gg \rightarrow H) &= (1 - \xi) \sigma_{NLO}^{SM}(gg \rightarrow H) & \text{MCHM4,} \\ \sigma_{NLO}(gg \rightarrow H) &= \frac{(1-2\xi)^2}{(1-\xi)} \sigma_{NLO}^{SM}(gg \rightarrow H) & \text{MCHM5.} \end{aligned} \quad (20)$$

The NLO SM gluon-fusion cross-section has been obtained with the program HIGLU [40].

W/Z boson fusion The next-important SM Higgs boson production cross-sections are the W and Z boson-fusion processes $qq \rightarrow qq + W^*W^*/Z^*Z^* \rightarrow qqH$ [41]. They also play a role for Higgs boson searches in the intermediate mass range, since the additional forward jets allow for a powerful reduction of the background processes. The NLO QCD corrections are of order 10% of the total cross-section [31,42]. The full NLO QCD and EW corrections to the differential cross-sections result in modifications of the relevant distributions by up to

⁸Equations (20) agree with the results obtained in Ref. [6], which confirms the claim of footnote 5 that all the corrections to the $H\gamma\gamma$ and Hgg vertices originate from the modified Yukawa interactions.

20% [43].

We have calculated the Higgs boson production in gauge boson fusion at NLO QCD, which is the approximation used in the ATLAS and CMS analyses. Since the QCD corrections do not involve Higgs interactions, the NLO QCD production cross-section for the composite Higgs model can be obtained from the SM NLO QCD process by multiplication with the same rescaling factor as for the Higgs gauge coupling squared [see Eq. (7)], i.e.,

$$\sigma_{NLO}(qqH) = (1 - \xi) \sigma_{NLO}^{SM}(qqH) \quad \text{for MCHM4 and MCHM5} . \quad (21)$$

We have obtained the SM production cross-section at NLO with the program VV2H [44].

Higgs-strahlung The Higgs-strahlung off W, Z bosons $q\bar{q} \rightarrow Z^*/W^* \rightarrow H + Z/W$ provides alternative production modes in the intermediate mass range $M_H \lesssim 2M_Z$ [45]. The NLO QCD corrections are positive and of $\mathcal{O}(30\%)$ [31, 46] while the NNLO corrections are small [47]. The full EW corrections are known and decrease the total cross-section by $\mathcal{O}(5-10\%)$ [48].

The NLO QCD corrections do not involve the Higgs couplings, so that the composite Higgs-strahlung cross-section at NLO QCD is obtained from the corresponding SM cross-section by the same rescaling factor as for the Higgs gauge boson coupling squared:

$$\sigma_{NLO}(VH) = (1 - \xi) \sigma_{NLO}^{SM}(VH) \quad \text{for MCHM4 and MCHM5} , \quad (22)$$

where V denotes W, Z . The NLO QCD SM Higgs-strahlung cross-section has been obtained with the program V2HV [44].

Higgs radiation off top quarks plays a role only for the production of a light SM Higgs boson with masses below ~ 150 GeV. The LO cross-section [49] is moderately increased ($\sim 20\%$) at the LHC by the NLO QCD corrections [50]. The production of a composite Higgs boson in association with a top quark pair at NLO QCD is obtained from the SM cross-section via

$$\begin{aligned} \sigma_{NLO}(Ht\bar{t}) &= (1 - \xi) \sigma_{NLO}^{SM}(Ht\bar{t}) && \text{MCHM4,} \\ \sigma_{NLO}(Ht\bar{t}) &= \frac{(1-2\xi)^2}{(1-\xi)} \sigma_{NLO}^{SM}(Ht\bar{t}) && \text{MCHM5.} \end{aligned} \quad (23)$$

The LO SM cross-section has been obtained by means of the program HQQ [44]. Subsequently it has been dressed with the K -factor quantifying the increase of the SM cross-section due to NLO corrections. In MCHM5, this cross-section may provide an interesting search channel for large values of ξ near one, where the enhancement factor compared to the SM cross-section becomes significant.

In MCHM4, all Higgs production cross-sections are reduced by the overall factor $(1 - \xi)$. We do not show these cross-sections separately since they can easily be obtained from the SM results, which are shown in Fig. 7 upper left. In order to make contact with the existing ATLAS and CMS experimental analyses of SM Higgs searches we use $\sqrt{s} = 14$ TeV, even if this is beyond the value the LHC will be able to reach in its first years of running. The production cross-sections in MCHM5 are also shown in Fig. 7, as a function of the Higgs boson mass in the interesting mass

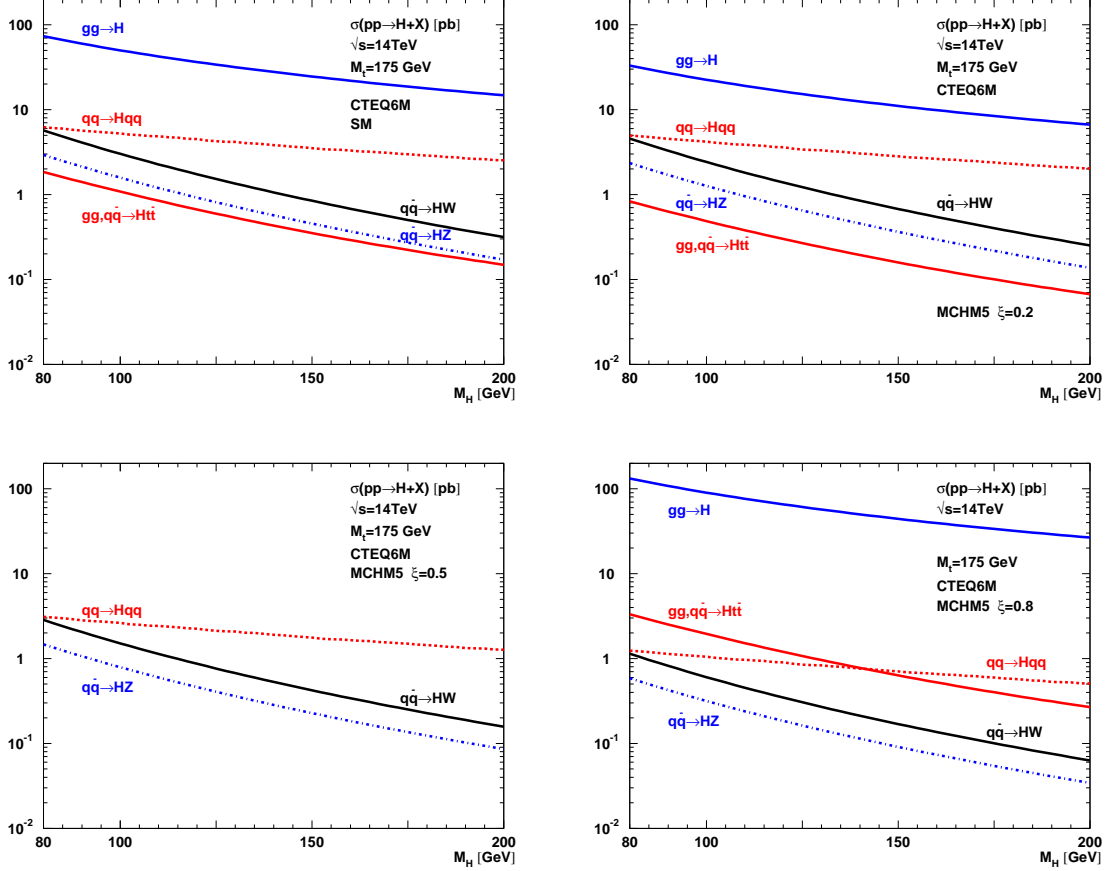


Figure 7: The LHC Higgs boson production cross-sections as a function of the Higgs boson mass in the SM ($\xi = 0$, upper left) and for MCHM5 with $\xi = 0.2$ (upper right), 0.5 (bottom left) and 0.8 (bottom right).

range $M_H = 80 \div 200$ GeV for $\xi = 0.2, 0.5$ and 0.8 . In the SM, the main production is given by gluon fusion, followed by gauge boson fusion. The Higgs-strahlung processes HW, HZ and the production in association with top quarks are less important. For $\xi = 0.2$ the processes involving quarks, i.e., gluon fusion and $t\bar{t}H$ production, are reduced by a factor 0.45 and the gauge boson processes, WW, ZZ fusion and Higgs-strahlung HW, HZ , are multiplied by a factor 0.8 , according to Eqs. (20) to (23). The inclusive Higgs production will hence shrink considerably and might render the Higgs searches difficult. The situation gets worse for $\xi = 0.5$, where the gluon fusion and $t\bar{t}H$ processes are completely absent and the gauge production processes are diminished by a factor 2 . For $\xi = 0.8$, on the other hand, the situation is reversed: while the gauge boson fusion and Higgs-strahlung processes are only 20% of the corresponding SM production processes and might eventually not be exploitable for Higgs boson searches, the gluon fusion and $t\bar{t}H$ production are enhanced by a factor 1.8 .

4.2 Statistical significances for different search channels

In order to obtain the significances for the most important Higgs boson search channels at the LHC, we refer to the analyses presented in the CMS TDR [51]. Referring to the ATLAS TDR

analyses [52] would not lead to very different results. The derivation of the significances in the composite Higgs models is drastically simplified by the fact that in our models we assumed only the couplings of the Higgs bosons to deviate from the SM. Therefore only the numbers of the signal events are modified while the numbers of the background events do not change. More precisely, we proceed as follows. The experimental analyses obtain the signal and background numbers in the investigated Higgs boson search channels after application of cuts. We take the signal numbers and rescale them according to our model. The rescaling factor \varkappa is dictated by the change in the production cross-sections and branching ratios compared to the Standard Model. For the composite Higgs production in the process p with subsequent decay into a final state X , this factor is then given by

$$\varkappa = \frac{\sigma_p BR(H \rightarrow X)}{\sigma_p^{SM} BR(H^{SM} \rightarrow X)} . \quad (24)$$

The number of signal events s is obtained from

$$s = \varkappa \cdot s^{SM} , \quad (25)$$

where we take the number of SM model signal events after application of all cuts, s^{SM} , from the experimental analyses. The signal events s and the background events after cuts, i.e., $b \equiv b^{SM}$ are used to calculate the corresponding significances in the composite Higgs model.

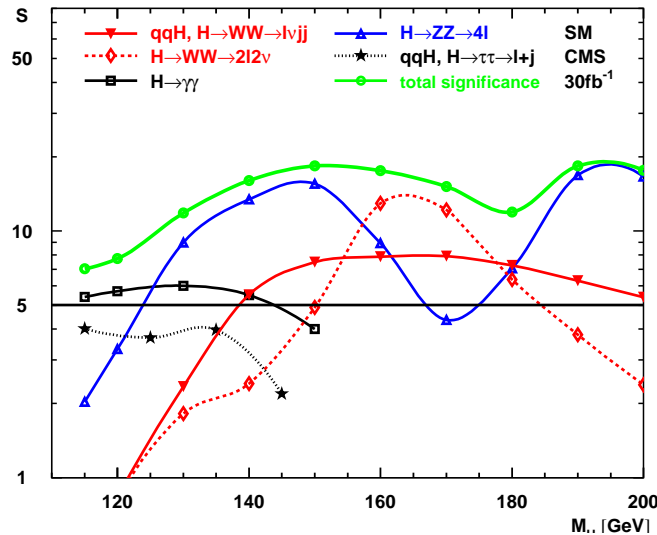


Figure 8: The significances in different Higgs search channels as a function of the Higgs boson mass in the SM with $\int \mathcal{L} = 30 \text{ fb}^{-1}$ and a CMS-type of analysis. The significances are computed using the data given in Tables 1–5, they will slightly differ from the *official* CMS numbers which rely on a more sophisticated statistical analysis.

Figure 8 shows for reference the significances of different channels searching for a light SM Higgs boson at CMS, as a function of $M_H = 115 \div 200 \text{ GeV}$ with $\int \mathcal{L} = 30 \text{ fb}^{-1}$. The gold-plated channel with 4 leptons in the final state from the Higgs decay into Z bosons reaches significances above 5 standard deviations for Higgs masses $\gtrsim 125 \text{ GeV}$. For Higgs masses around the W boson threshold

inclusive production with subsequent decay into W bosons takes over. Higgs production in vector boson fusion, with decay into WW , provides an efficient search channel in the intermediate region $\sim 140 \div 180$ GeV. The light Higgs mass region below ~ 120 GeV turns out to be more difficult. Sophisticated cuts and combination of several search channels are needed to achieve significances above 5σ . In this way, the LHC will be able to cover the whole canonical Higgs mass range up to ~ 600 GeV (not shown in the plot). The ATLAS experiment provides a similar coverage. We take these SM results as a benchmark and study how the modified couplings of a composite Higgs will change this picture. The channels we investigate are

$$\begin{aligned}
&\text{Inclusive production with subsequent decay : } H \rightarrow \gamma\gamma \\
&\quad H \rightarrow ZZ \rightarrow 2e2\mu, 4e, 4\mu \\
&\quad H \rightarrow WW \rightarrow 2l2\nu \\
&\text{Vector boson fusion with subsequent decay : } H \rightarrow WW \rightarrow l\nu jj \\
&\quad H \rightarrow \tau\tau \rightarrow l + j + E_T^{\text{miss}}.
\end{aligned} \tag{26}$$

We do not consider other Higgs channels which are of subleading importance. For example, we do not discuss $t\bar{t}H$ production with subsequent decay into $b\bar{b}$. This channel has been removed recently from the list of possible search modes, since controlling the background appears to be too difficult to make reliable predictions. We have also checked that we do not gain much significance by the inclusion of the gluon-fusion Higgs production followed by $H \rightarrow \tau\tau$ decay, with an additional resolved jet ($pp \rightarrow H + j \rightarrow \tau\tau + j$) [53], which has been recently revived in [54] as a promising channel for light Higgs searches in models with an enhanced Higgs BR into $\tau\tau$. In our models, whenever this channel has a sizeable significance, other channels already provide large significance.

In the following, we will discuss each channel in turn, giving the expected significance as a function of the Higgs mass M_H and the ξ parameter. For concreteness, we fix the integrated luminosity to $\int \mathcal{L} = 30 \text{ fb}^{-1}$. We base ourselves on the CMS TDR [51] and the relevant CMS Notes. Similar results would be expected for ATLAS.

Since the CMS analyses calculate the significances with different definitions for the various channels, we take the pragmatic approach to get our $\xi = 0$ significances as close as possible to the SM result given by CMS, so that any deviation at $\xi \neq 0$ can be attributed to the composite character of the Higgs. We are forced then to choose different significance definitions (as listed in the appendix). Our combined significances have been obtained by adding in quadrature the individual significances without caring about their heterogeneous nature and, therefore, have to be taken as merely indicative.

4.3 $H \rightarrow \gamma\gamma$

This channel is of crucial importance for the Higgs search at low masses (below ~ 150 GeV, see Fig. 8) where the decays into real gauge bosons are closed. Furthermore, since the decay into photons is loop-mediated, it is sensitive to new physics effects due to new particles in the loop (see Ref. [16] for a recent study). The signature is characterized by two isolated high E_T photons. While the photons can easily be identified, this channel is very challenging due to the small signal rate compared to the large background. The reason is that the Higgs boson dominantly decays into $b\bar{b}$ in this mass region, which cannot be exploited though due to the high QCD background. The $\gamma\gamma$ signal will appear as a narrow mass peak above the large background. The latter can be measured from the sidebands outside the peak and extrapolated into the signal region.

For the production cross-sections, we use the same as in the CMS analyses⁹ which are based on the Higgs production in gluon fusion, vector boson fusion, associated production with W, Z bosons and $Ht\bar{t}$ production. As SM benchmark data for the expected significance we use the CMS standard cut-based analysis, see Table 1, which subdivides the total sample of events in a number of different categories especially designed to improve the combined significance. A more sophisticated analysis [51] leads to even higher significances and our results for this channel are therefore conservative.

M_H (GeV)	115	120	130	140	150
S_{CMS}	5.4	5.7	6.0	5.5	4.0

Table 1: Expected significances for the SM Higgs search in the $H \rightarrow \gamma\gamma$ channel, with $\int \mathcal{L} = 30 \text{ fb}^{-1}$, as given by the standard CMS cut-based analysis presented in Ref. [55], Fig. 5.

At the different steps of this analysis the partial significances of the different categories are well described by the simple formula $s_i/\sqrt{b_i}$ so that the analysis for the composite Higgs can be performed exactly in the same way, except for an overall universal factor that takes into account the change in the signal yields, so that the combined total significance is rescaled by that same universal factor. While a dedicated CMS-type cut-based analysis for the composite Higgs case could improve over the rescaled significance, this simple recipe allows us to make smooth contact with the CMS results and to improve over simpler significance estimates which use the total number of signal and background events.

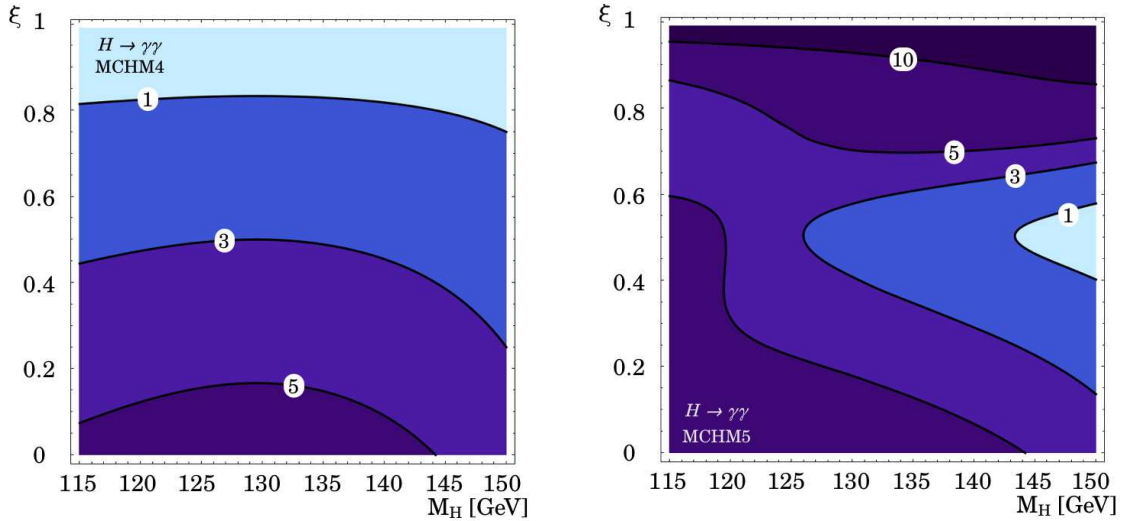


Figure 9: The signal significance in the channel $H \rightarrow \gamma\gamma$ in the (M_H, ξ) plane with an integrated luminosity of 30 fb^{-1} for MCHM4 (left) and MCHM5 (right). The darker the color, the higher the significance. The contours delineate the regions corresponding to a significance of 1, 3, 5 and 10σ .

The results for the significances in both MCHM4 and MCHM5 are presented in Fig. 9 as contour lines in the plane (M_H, ξ) . The values along the $\xi = 0$ axis coincide with the SM numbers as given

⁹See section 2.1 of the CMS TDR [51] and the CMS Note 2006/112 [55].

in Table 1. In MCHM4 (left plot), the significance degrades quickly as ξ gets larger as a result of the production cross-section getting smaller with the decreasing rescaling factor $(1 - \xi)$ (we remind the reader, that in MCHM4 the branching ratios do not change compared to the SM). This trend will recur in all channels. In MCHM5 (right plot), the significance is worst along intermediate values of ξ where the total production cross-section has a minimum, although this effect is partially compensated at low Higgs masses by the increase in the $H \rightarrow \gamma\gamma$ branching ratio in this ξ region, see Figs. 1 and 7. Both behaviours are due to the vanishing Yukawa couplings at $\xi = 0.5$. The expected significance is larger than 5σ in a large region of parameter space, especially for ξ near 1, where the production cross-sections mediated via Yukawa couplings are largely enhanced. Here the significances can be larger than those of the SM.

4.4 $H \rightarrow ZZ \rightarrow 4l$

This clean channel, with the Higgs decaying through $ZZ^{(*)}$ into $4e$, $2e2\mu$ and 4μ , is one of the most promising Higgs discovery channels for Higgs masses above ~ 130 GeV, although, as shown in Fig. 8, the expected significance drops in the neighbourhood of $M_H \sim 160$ GeV where $H \rightarrow WW$ peaks (see Fig. 1). The production cross-section, dominated by gluon fusion in this mass range, is large and so is the branching ratio into $ZZ^{(*)}$ which is sizeable for $M_H \gtrsim 130$ GeV. The channel yields a significant, very clean and simple multi-lepton final state signature. Furthermore, it provides a precise determination of the Higgs boson mass and, to a lesser extent, cross-section and also allows, via angular and mass distributions, the determination of the spin and CP quantum numbers of the Higgs boson [56, 57].

The CMS analyses¹⁰ are based on the production through gluon fusion and vector boson fusion. The Higgs boson signal is characterized by two pairs of isolated primary electrons and muons. One pair in general results from a Z boson decay on its mass shell. In the analyses the main background processes considered are $t\bar{t}, Zb\bar{b} \rightarrow 2l\bar{b}\bar{b}$ and $ZZ \rightarrow 4l$. In order to extract the expected experimental sensitivity a sequential cut based approach is used and the search is performed with a window in the hypothetical mass M_H . The SM signal and background rates as well as the significances are given in Table 2. The resulting significances are very similar in the three different subchannels (both in the SM and in the composite Higgs models) so that we only discuss the significance for the combined channels, which is shown in Fig. 8 for the SM. For the calculation of the composite Higgs significances with 30 fb^{-1} integrated luminosity, we use the Poisson significance S_P as defined in the appendix, neglecting the systematic uncertainty of the background, which has only a small effect.

The significances for both MCHM4 and MCHM5 are presented in Fig. 10 as contour lines in the plane (M_H, ξ) . The values along the $\xi = 0$ axis coincide with the SM numbers scaled up to 30 fb^{-1} . In MCHM4 (left plot), the significance degrades as usual with increasing ξ due to the reduction in the production cross-section but remains sizeable up to large values of ξ due to its initially large value at $\xi = 0$. In MCHM5 (right plot), the significance follows in its horizontal behaviour the SM change in the significance with the Higgs mass. The vertical behaviour as function of ξ results mostly from the variation of the cross-sections with ξ which drops considerably at $\xi = 0.5$ where

¹⁰We used Section 2.2 of the CMS TDR [51] and CMS Note 2006/115 [58] (for $4e$); Section 3.1 of the CMS TDR and CMS Note 2006/122 [59] (for 4μ); Section 10.2.1 of the CMS TDR and CMS Note 2006/136 [60] (for $2e2\mu$); and the more recent CMS PAS HIG-08-003 [61].

M_H (GeV)	115	120	130	140	150	160	170	180	190	200
s	0.18	0.33	1.27	2.43	3.05	1.51	0.73	1.78	6.5	7.08
b	0.16	0.19	0.29	0.42	0.47	0.47	0.61	1.38	2.74	3.52
S_{CMS}	—	0.13	1.32	2.22	2.64	1.36	0.50	1.09	2.92	2.87
S_P	—	0.13	1.35	2.24	2.64	1.38	0.50	1.09	2.96	2.92

Table 2: Number of signal s and background events b and resulting significance S_{CMS} expected for the SM Higgs search in the channel $H \rightarrow ZZ \rightarrow 2l2l'$, with $\int \mathcal{L} = 1 \text{ fb}^{-1}$, as given in Ref. [61], Table 3. To extend the Higgs mass range, the point $M_H = 115 \text{ GeV}$ has been added using results from refs. [58–60]. For comparison, the last row gives the expected Poisson significance S_P for $\int \mathcal{L} = 1 \text{ fb}^{-1}$, with systematic background uncertainties Δb included (as defined in the appendix), and with $\Delta b/b = 0.21$ (0.08), for low (high) Higgs masses.

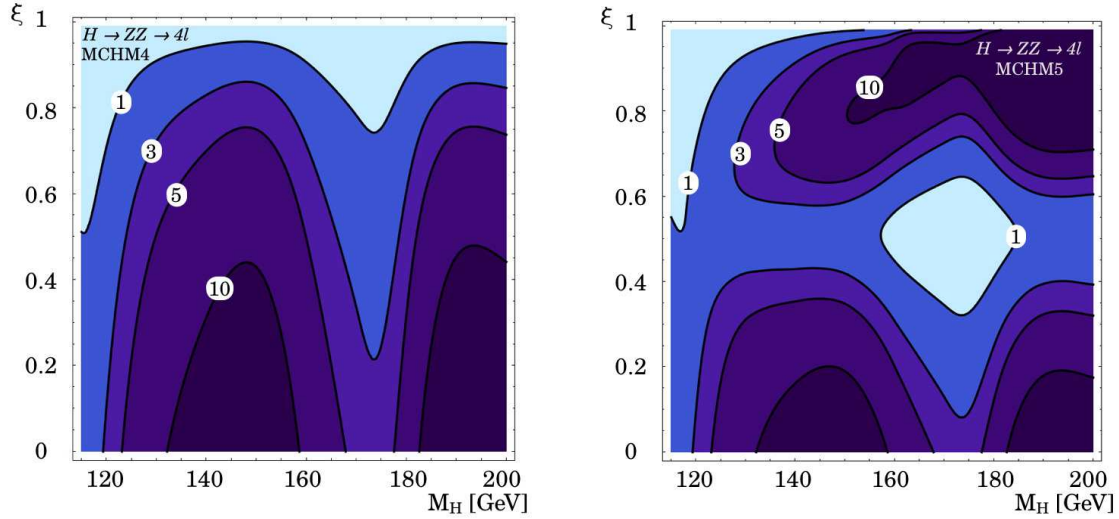


Figure 10: The combined signal significance for the channels $H \rightarrow ZZ \rightarrow 4l$ in the (M_H, ξ) plane with an integrated luminosity of 30 fb^{-1} for MCHM4 (left) and MCHM5 (right). The darker the color, the higher the significance. The contours correspond to a significance of 1, 3, 5 and 10σ .

the Yukawa couplings are zero. The drop is partially compensated by the enhancement in the ZZ branching ratio in this region (see Figs. 1 and 7). Thus the significance is worst along intermediate values of ξ and higher for large values of ξ where the gluon-fusion cross-section is enhanced. Here it can even exceed the SM significance for Higgs mass values above $\sim 180 \text{ GeV}$.

4.5 $H \rightarrow WW \rightarrow 2l2\nu$

The Higgs decay into WW which subsequently decay into leptons is the main discovery channel in the intermediate region $2M_W \lesssim M_H \lesssim 2M_Z$ where the Higgs branching ratio into WW is close to one. This channel has seen its revival after it was realized that the spin correlation in the W^+W^- system can be exploited to extract the signal from the background [62]. The signature is characterized by two leptons and missing high energy. Since no narrow mass peak can be reconstructed, a good background control and a high signal to background ratio are needed. The

considered production mechanisms used in the CMS analyses¹¹ are both gluon fusion and vector boson fusion. The SM data for this channel are collected in Table 3. We use the *ScP2* significance (see the appendix) including a background systematic uncertainty estimated to be 14.6% at 1 fb⁻¹. The SM result for 30 fb⁻¹, with background systematic uncertainty scaled down to 10%, is shown in Fig. 8 (we calculate the significance simply from the total numbers of signal and background events. The CMS analysis is performed first with the *ee*, *eμ* and *μμ* subchannels separately which are then combined).

M_H (GeV)	120	130	140	150	160	170	180	190	200
s	7.5	17.3	31.4	24.4	67.5	66.8	50.9	31.2	29.6
b	87.3	89.4	121.4	42.5	37.4	40	67.3	73.3	115.8
S_{CMS}	0.55	1.0	1.55	2.4	5.93	6.1	3.35	1.95	1.45
$ScP2$	0.46	1.03	1.42	2.4	6.16	5.89	3.42	2.08	1.39

Table 3: Number of signal and background events and resulting significance expected for the SM Higgs search in the channel $H \rightarrow WW \rightarrow 2l2\nu$, with $\int \mathcal{L} = 1 \text{ fb}^{-1}$, as given in Ref. [64], Table 9 and Fig. 6. The last row gives the expected significance $ScP2(s, b, \Delta b)$ (as defined in the appendix), with $\Delta b/b = 0.146$ and for $\int \mathcal{L} = 1 \text{ fb}^{-1}$.

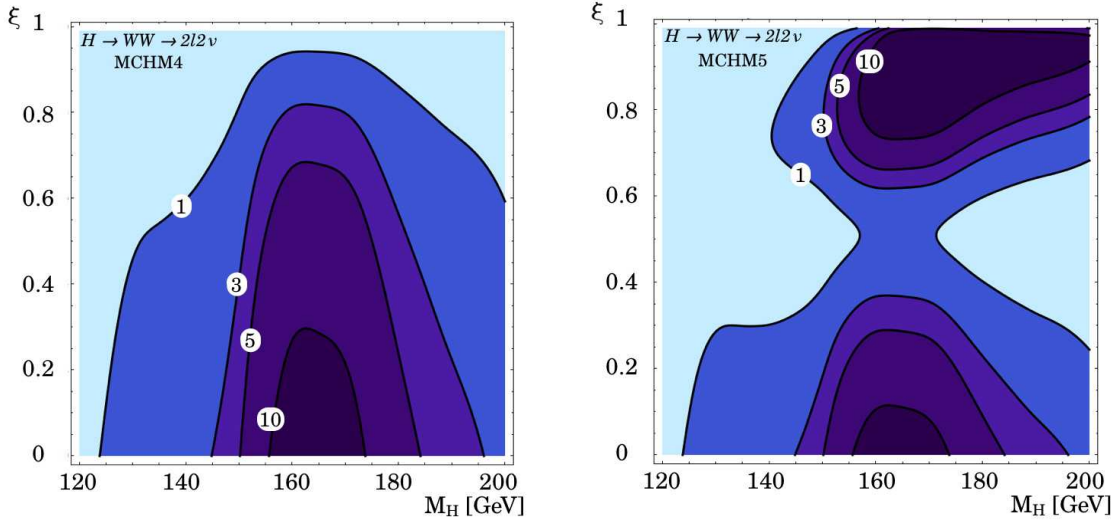


Figure 11: The signal significance in the channel $H \rightarrow WW \rightarrow 2l2\nu$ in the (M_H, ξ) plane with an integrated luminosity of 30 fb⁻¹ and 10% background systematic uncertainty for MCHM4 (left) and MCHM5 (right). The contours correspond to a significance of 1, 3, 5 and 10σ.

The results for the expected significances in MCHM4 and MCHM5 are presented in Fig. 11 as contour lines in the plane (M_H, ξ) . As usual, the values along $\xi = 0$ agree well with the CMS SM results. The significance in MCHM4 degrades with increasing ξ , but remains sizeable up to large values of ξ due to its initially large value at $\xi = 0$. The value of ξ at which the significance really deteriorates compared to the SM one depends on the Higgs mass. For MCHM5, we find the usual

¹¹The relevant CMS documents are Section 10.2.2 of the CMS TDR [51], the CMS Note 2006/047 [63] and the most recent CMS PAS HIG-08-006 [64].

behaviour, with the smallest significances at $\xi \sim 0.5$, the value that determines an approximate axis of symmetry for the resulting significances. As for the previous channels, the expected significance is larger than 5σ in a sizeable portion of parameter space and exceeds the SM significance at large values of ξ where the Yukawa couplings, and hence the gluon-fusion process, are significantly enhanced. These regions with largest significances, however, are already being probed and a priori excluded by the Tevatron (see Section 3), which exploits the same decay channel.

4.6 $H \rightarrow WW \rightarrow l\nu jj$

The Higgs search in vector boson fusion with subsequent decay $H \rightarrow W^+W^- \rightarrow l^\pm\nu jj$ is very important to cover the Higgs mass region $160 \text{ GeV} \lesssim M_H \lesssim 180 \text{ GeV}$ where the $H \rightarrow ZZ^*$ branching ratio is largely suppressed because of the opening of $H \rightarrow W^+W^-$. Due to the possibility of direct Higgs mass reconstruction, it complements the previous search channel, which has two unobservable neutrinos in the final state. The event topology is characterized by two forward jets, two central jets from the W hadronic decay, and one high p_T lepton and missing transverse energy from the W leptonic decay. Furthermore, an extra jet veto can be applied to efficiently reduce the background. The large background necessitates robust reconstruction and selection strategies to extract the signal from the background and minimize the systematic uncertainties. The SM data for this channel are collected in Table 4¹². For the calculation of the significances in the composite models, we use the ScL' significance (see the appendix) including a background systematic uncertainty of 16%. The SM result at 30 fb^{-1} is shown in Fig. 8. The significance is larger than 5σ for $M_H \gtrsim 135 \text{ GeV}$.

$M_H \text{ (GeV)}$	120	130	140	150	160	170	180	190	200
s	6.93	19.92	49.68	69.51	89.67	90.18	82.14	70.2	59.49
b	34.92	34.92	34.92	34.92	46.95	46.95	46.95	46.95	46.95
S_{CMS}	0.8	2.25	5.3	7.3	8.1	8.15	7.3	6.25	5.3
ScL'	0.84	2.34	5.52	7.47	7.86	7.90	7.26	6.29	5.4

Table 4: Number of signal and background events and resulting significance expected for the SM Higgs search in the channel $H \rightarrow WW \rightarrow l\nu jj$, at $\int \mathcal{L} = 30 \text{ fb}^{-1}$ with full extra jet veto, as given in Section 10.2.4 of the CMS TDR [51], Tables 10.12, 10.13 (rescaling the integrated luminosity) and Fig. 10.19. The last row gives the expected significance $ScL'(s, b, \Delta b)$ (as defined in the appendix) with $\Delta b/b = 0.16$ and for $\int \mathcal{L} = 30 \text{ fb}^{-1}$.

The results for the expected significances in MCHM4 and MCHM5 are presented in Fig. 12 as contour lines in the plane (M_H, ξ) . As usual, the values along $\xi = 0$ agree well with the CMS SM results. The significance in MCHM4 degrades with increasing ξ but remains sizeable up to large values of ξ due to its initially large value at $\xi = 0$. The significance never exceeds the SM significance. Due to the fact that only vector boson fusion (which is always suppressed compared to the SM cross-section) production is considered, MCHM5 does not exhibit the usual symmetric behaviour around the axis $\xi = 0.5$. The behaviour is quite similar to that in MCHM4 with the differences that, in MCHM5, the regions with higher significance are larger for low ξ values, but smaller for values of $\xi \gtrsim 0.6$. The former is due to the enhanced branching ratio into WW in

¹²The relevant CMS documents are Section 10.2.4 of the CMS TDR [51] and the CMS Note 2006/092 [65].

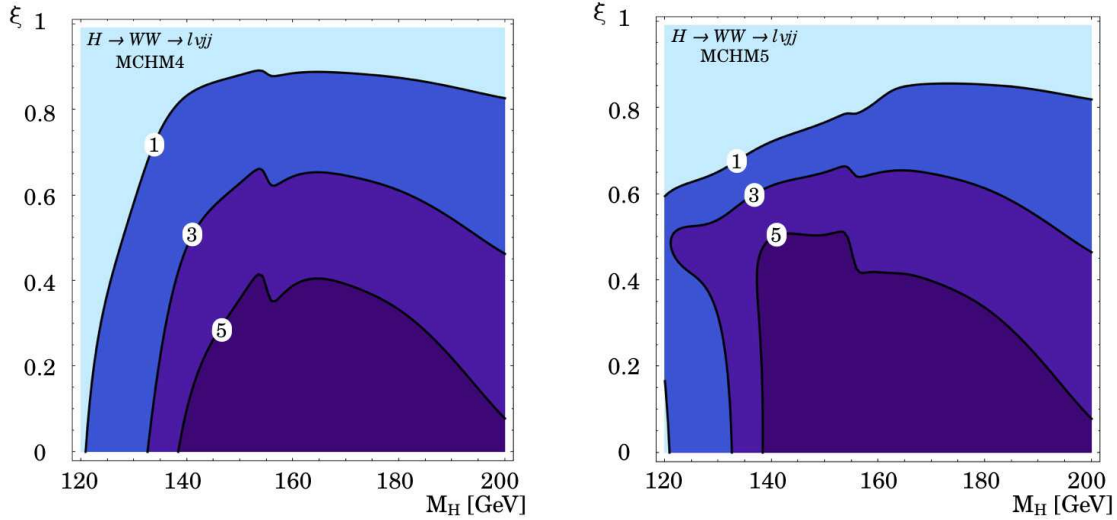


Figure 12: The signal significance in the channel $H \rightarrow WW \rightarrow l\nu jj$ in the (M_H, ξ) plane with an integrated luminosity of 30 fb^{-1} and 16% background systematic uncertainty for MCHM4 (left) and MCHM5 (right). The contours correspond to a significance of 1, 3, 5 and 10σ .

MCHM5, reaching its maximum at $\xi = 0.5$ where the Yukawa decay channel into $b\bar{b}$ is closed. The latter is due to the suppressed branching ratio into WW for values of ξ beyond 0.5, where in turn the decay into $b\bar{b}$ is enhanced.

Two regions are worthwhile discussing in more detail. Both MCHM4 and MCHM5 exhibit an edge in the significance around $M_H \approx 150 \text{ GeV}$. This is due to the larger background values used in the CMS analyses for $M_H \geq 160 \text{ GeV}$ (due to a different hadronic W mass selection window for $M_H < 160 \text{ GeV}$). Finally, MCHM5 shows a bulge with higher luminosity around $\xi \sim 0.5$ extending to lower Higgs mass values. This is due to the enhanced branching ratio into WW for $\xi = 0.5$. Altogether the expected significance is at most as good as in the SM and larger than 5σ only for $\xi < 0.5$.

4.7 $H \rightarrow \tau\tau \rightarrow l + j + E_T^{\text{miss}}$

In parton-level analyses [66], as well as in studies with detector simulation [67], it was shown that Higgs production in vector boson fusion with subsequent decay into τ leptons is an important search channel at low Higgs masses, $M_H \lesssim 140 \text{ GeV}$. In this mass region the $H \rightarrow \tau\tau$ decay is second in importance after the $b\bar{b}$ decay (which cannot be exploited because of the large QCD background). Although this is not the main channel in that region, it can contribute to improve the total significance when combined with other channels. Furthermore this channel adds to the determination of the Higgs couplings [66].

The signature of the signal process are a high p_T lepton and a τ -jet, two energetic forward jets and the total missing E_T of the system. The backgrounds considered in the analysis¹³ are the irreducible ones from QCD and electroweak Z/γ^* boson production with 2 or 3 associated jets and the reducible background processes from W + multi-jet and $t\bar{t}$ events. The background can

¹³The relevant CMS documents are Section 10.2.3 of the CMS TDR [51], the CMS Note 2006/088 [68].

efficiently be reduced by using the characteristics of the weak boson fusion process, which are the wide rapidity separation of the two leading quark jets and the suppressed hadronic activity in the central region due to the absence of colour exchange between the forward quark jets. The SM data for this channel are collected in Table 5. We use the Poisson significance (see the appendix) including a background systematic uncertainty estimated to be 7.8%. The SM result is shown in Fig. 8.

M_H (GeV)	115	125	135	145
s	10.5	7.8	7.9	3.6
b	3.7	2.2	1.8	1.4
S_{CMS}	3.97	3.67	3.94	2.18
S_P	4.01	3.70	3.97	2.19

Table 5: Number of signal and background events and resulting significance expected for the SM Higgs search in the channel $H \rightarrow \tau\tau \rightarrow l + j + E_T^{miss}$, with $\int \mathcal{L} = 30 \text{ fb}^{-1}$ as given in Section 10.2.3 of the CMS TDR [51], Table 10.10. The last row gives the expected Poisson significance S_P (as defined in the appendix) with $\Delta b/b = 0.078$ and for $\int \mathcal{L} = 30 \text{ fb}^{-1}$.

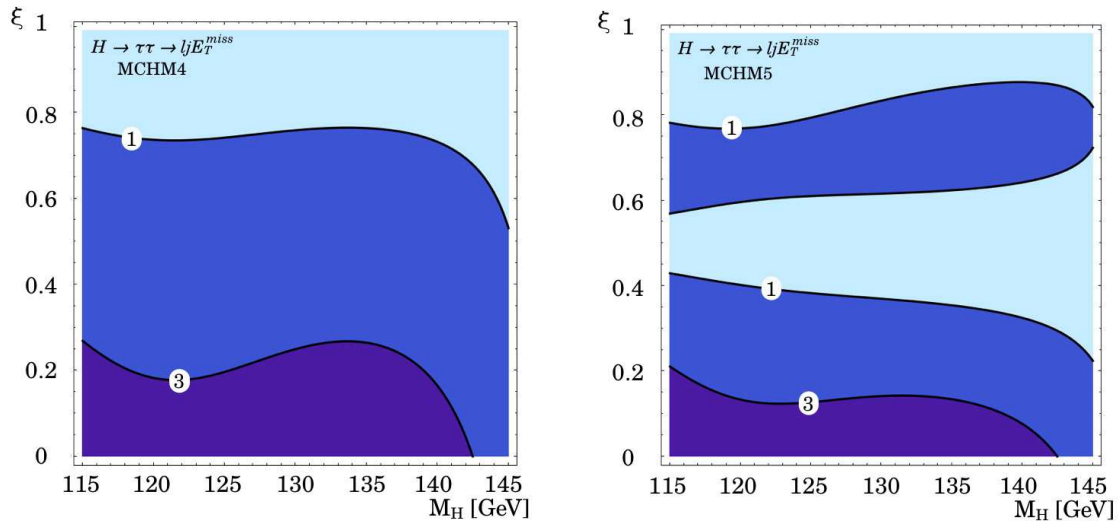


Figure 13: The signal significance in the channel $H \rightarrow \tau\tau \rightarrow l + j + E_T^{miss}$ in the (M_H, ξ) plane with an integrated luminosity of 30 fb^{-1} and 7.8% background systematic uncertainty for MCHM4 (left) and MCHM5 (right). The contours correspond to a significance of 1, 3 and 5σ .

The results for the expected significances in MCHM4 and MCHM5 are presented in Fig. 13 as contour lines in the plane (M_H, ξ) . As usual, the values along $\xi = 0$ agree well with the CMS SM results. The significance in MCHM4 degrades with increasing ξ . MCHM5 produces a similar decrease in significance, since only vector boson fusion production is considered¹⁴. For $\xi \lesssim 0.6$ the significance is lower than in MCHM4 because of the suppressed branching ratio into $\tau\tau$ which vanishes finally at $\xi = 0.5$. Beyond this value it increases with rising ξ so that at high ξ values,

¹⁴In this region with $\xi \sim 1$ the gluon-fusion process $pp \rightarrow H + j \rightarrow \tau\tau + j$ of Refs. [53, 54] would be important. Nevertheless, this region is already covered by the channel $H \rightarrow ZZ \rightarrow 2l2l'$.

MCHM4 and MCHM5 show a similar behaviour. Unlike in the previous channels, the expected significances in both models are always less than 5σ , since already in the SM the significances range below this value. MCHM4 and MCHM5 cannot compensate for that as with the vector boson fusion process the production cross-section is always smaller than in the SM and the increase in the branching ratio into $\tau\tau$ in MCHM5 cannot keep up with that.

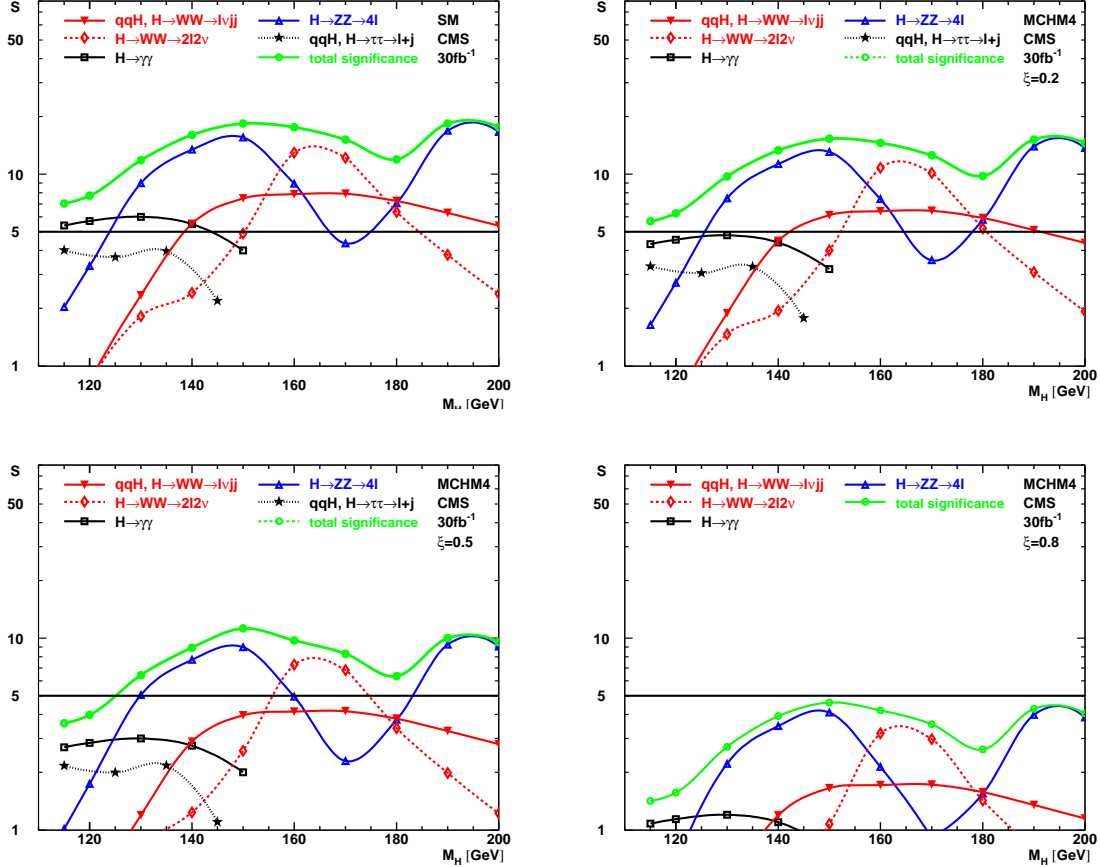


Figure 14: The significances in different channels as a function of the Higgs boson mass in the SM ($\xi = 0$, upper left) and for MCHM4 with $\xi = 0.2$ (upper right), 0.5 (bottom left) and 0.8 (bottom right).

5 Summary of results and conclusions

Combining the various channels discussed in the previous section gives an overall view of the expected significances and interplay of the different search channels we have discussed. Figures 14 and 15 summarize the situation in MCHM4 and MCHM5, respectively, presenting as a function of M_H the different expected significances and the total combined one. We choose the three representative values $\xi = 0.2, 0.5$ and 0.8 and also show the SM case ($\xi = 0$) for comparison.

In both models, for $\xi = 0.2$ the expectations are less promising than in the SM. Both the gluon fusion and the gauge boson fusion production cross-sections are reduced, so that all the significances move downwards. Also, in MCHM5, this cannot be compensated by the enhancement of the branching ratios into $\gamma\gamma$ and massive gauge bosons. The overall significance in MCHM5 is

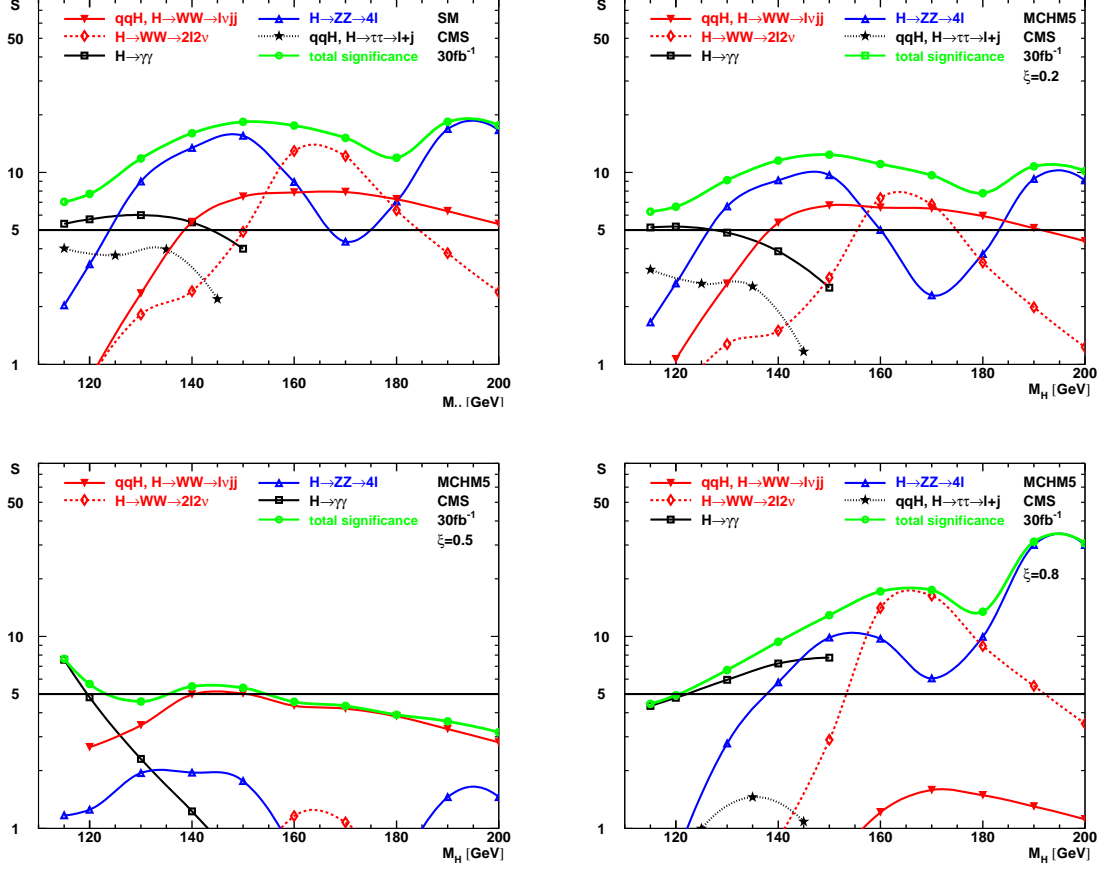


Figure 15: The significances in different channels as a function of the Higgs boson mass in the SM ($\xi = 0$, upper left) and for MCHM5 with $\xi = 0.2$ (upper right), 0.5 (bottom left) and 0.8 (bottom right).

worse than in MCHM4 because the gluon-fusion process, which contributes to the main channels $H \rightarrow ZZ \rightarrow 4l$ and $H \rightarrow WW \rightarrow 2l2\nu$, is more strongly suppressed than in MCHM4. Nevertheless, by combining several search modes, discovery with an integrated luminosity of 30 fb^{-1} will still be possible.

The situation looks worse for $\xi = 0.5$. In MCHM4, the combined significance drops below 5σ for the interesting range $M_H \lesssim 125 \text{ GeV}$. A more sophisticated treatment of the $H \rightarrow \gamma\gamma$ channel (like the one performed by CMS [51]) would be required to improve the significance in that region, or other alternative search channels should be exploited (see below). In MCHM5, the combined significance is much worse (as the inclusive production cannot be exploited here anymore) and barely reaches 5σ in some ranges, although these include the interesting low mass range, thanks to the enhanced Higgs branching ratio into photons. In fact, this channel seems to be good for searches for Higgs masses below 120 GeV , as the tendency of the curve implies. However, in order to confirm this, experimental analyses for masses below 115 GeV , which are not yet excluded in the composite model, would be needed. For higher masses only the weak boson fusion with subsequent decay into WW can be exploited.

For $\xi = 0.8$, the situation is totally different in the two models. In MCHM4, the progressive de-

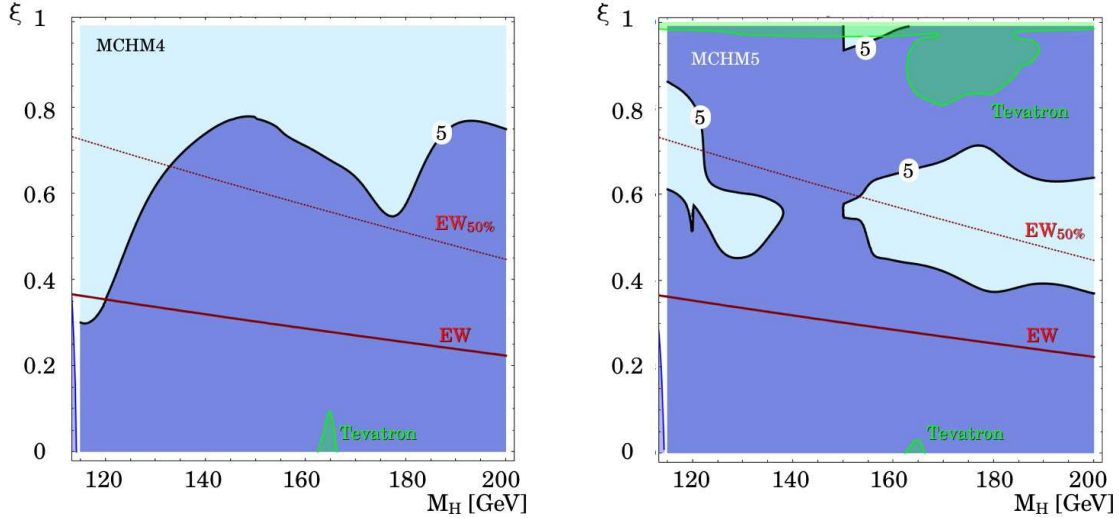


Figure 16: The total 5σ significance for the combined channels in the (M_H, ξ) plane with an integrated luminosity of 30 fb^{-1} for MCHM4 (left) and MCHM5 (right), as in the previous figures the darker region corresponds to the higher significance. The Tevatron exclusion bounds (green) from Section 3 are also reported. The red continuous line delineates the region favored at 99% CL (with a cutoff scale fixed at 2.5 TeV) while the region below the red dashed line survives if there is an additional 50% cancellation of the oblique parameters. The LEP exclusion bounds are only marginally visible (tiny blue region in the bottom left corner) since the search analyses carried out by CMS deal exclusively with Higgs masses above the SM LEP exclusion bound.

terioration of the significance continues and the combined significance is always below 5σ . Instead, for MCHM5, things look much better for masses above ~ 120 GeV. The production is completely taken over by the gluon-fusion process and leads to large significances in the massive gauge boson final states. Also the $\gamma\gamma$ final state contributes significantly above ~ 120 GeV. The tendency of the curve shows that, for masses above 150 GeV, this channel will still have large significance. However, also here experimental analyses are needed to confirm this. At low masses, the situation does not look as good. Since the vector boson fusion and Higgs-strahlung processes are largely suppressed they cannot contribute to the search channels in this difficult region. One has to rely on inclusive production with subsequent decay into photons. Besides an improved analysis of the $H \rightarrow \gamma\gamma$ mode, perhaps $t\bar{t}H$ production with $H \rightarrow b\bar{b}$ might help. Although, as we said, this channel is no longer considered to be very useful in the SM, the enhancement of the gluon-fusion cross-section (by a factor 1.8 for $\xi = 0.8$) might reopen this option.

Figure 16 gives the 5σ -significance contour line in the plane (M_H, ξ) for MCHM4 and MCHM5. Most of the CMS analyses available did not consider Higgs mass below the SM LEP exclusion bound. However, by comparing Fig. 5 and Fig. 16, we can infer that it might be worth extending these analyses for lower values of the Higgs mass, in particular in the region $\xi \sim 0.5$, where the LEP exclusion limit really deteriorates and the conflict with EW precision measurements is still not too severe.

In summary, the search modes and corresponding significances can substantially depart from the SM case, even at moderately low value of ξ , i.e., for large compositeness scale of the Higgs boson. We did not perform a full exploration of the 2D parameter space that controls the deviations of

the Higgs couplings, but, focusing on two particular directions in this parameter space, we have identified interesting and distinctive behaviors. In the first explicit model we consider, all the Higgs couplings are reduced compared to the SM ones and, as a result, the Higgs searches deteriorate. On the contrary, in the second model, for low enough composite scales, the Higgs production by gluon fusion is enhanced and results in searches with higher statistical significances.

After more than 40 years of theoretical existence, the Higgs boson has a chance to show its face soon in the LHC detectors. Its discovery will certainly also provide us with useful information about the nature of the Higgs sector since the relative importance of the various production and decay channels measures, to a certain extent, the dynamics of this Higgs sector and will tell whether the force behind the phenomenon of electroweak symmetry breaking is weak or strong.

Appendix: Significance estimators

For a given number of expected signal and background events (s and b , respectively) there are many alternative ways in the literature to compute the corresponding expected significance, taking also into account the possible presence of a systematic uncertainty Δb on b (see [69] for a comparison of different possibilities). Besides the simple estimate s/\sqrt{b} , we make use in this paper of the following definitions of significance:

$$\begin{aligned} ScL[s, b] &\equiv \sqrt{2[(s+b)\log(1+s/b) - s]} , \\ ScL'[s, b, \Delta b] &\equiv ScL[s, b + \Delta b^2] , \end{aligned} \quad (27)$$

and

$$ScP2[s, b, \Delta b] \equiv 2 \left(\sqrt{s+b} - \sqrt{b} \right) \sqrt{\frac{b}{b + \Delta b^2}} . \quad (28)$$

Note that this last definition, advocated in Eq. (A.5) of Appendix A of the CMS TDR [51] is incorrectly written there [70].

Finally, the Poisson significance is defined as the number of standard deviations that a Gaussian variable would fluctuate in one direction to give the same p -value computed using the Poisson distribution given the numbers of signal and background events, i.e., the Poisson significance, S_P , is the solution of the equation

$$\sum_{i=0}^{s+b-1} \frac{e^{-b} b^i}{i!} = \int_{-\infty}^{S_P} dx \frac{e^{-x^2/2}}{\sqrt{2\pi}} . \quad (29)$$

Acknowledgments

We thank Alexander Belyaev, Roberto Contino, Javier Cuevas, Michael Dittmar, Abdelhak Djouadi, Tommaso Dorigo, Gian Giudice, Chiara Mariotti, Riccardo Rattazzi and Michael Spira for useful discussions and for providing relevant information. J.R.E. and M.M. thank CERN PH-TH for partial financial support. This work has been partly supported by the European Commission under the contract ERC advanced grant 226371 ‘MassTeV’, the contract PITN-GA-2009-237920 ‘UNILHC’, and the contract MRTN-CT-2006-035863 ‘ForcesUniverse’, as well as by the Spanish Consolider-Ingenio 2010 Programme CPAN (CSD2007-00042) and the Spanish Ministry MICNN under contract FPA 2007-60252.

References

- [1] G. F. Giudice, C. Grojean, A. Pomarol and R. Rattazzi, *JHEP* **0706** (2007) 045 [hep-ph/0703164].
- [2] R. Contino, C. Grojean, M. Moretti, F. Piccinini and R. Rattazzi, [hep-ph/1002.1011].
- [3] W. D. Goldberger, B. Grinstein and W. Skiba, *Phys. Rev. Lett.* **100** (2008) 111802 [hep-ph/0708.1463]; J. Fan, W. D. Goldberger, A. Ross and W. Skiba, *Phys. Rev. D* **79** (2009) 035017 [hep-ph/0803.2040]; L. Vecchi, [hep-ph/1002.1721].
- [4] D. B. Kaplan and H. Georgi, *Phys. Lett. B* **136** (1984) 183.
- [5] S. Dimopoulos and J. Preskill, *Nucl. Phys. B* **199**, 206 (1982); T. Banks, *Nucl. Phys. B* **243**, 125 (1984); D. B. Kaplan, H. Georgi and S. Dimopoulos, *Phys. Lett. B* **136**, 187 (1984); H. Georgi, D. B. Kaplan and P. Galison, *Phys. Lett. B* **143**, 152 (1984); H. Georgi and D. B. Kaplan, *Phys. Lett. B* **145**, 216 (1984); M. J. Dugan, H. Georgi and D. B. Kaplan, *Nucl. Phys. B* **254**, 299 (1985).
- [6] A. Falkowski, *Phys. Rev. D* **77** (2008) 055018 [hep-ph/0711.0828].
- [7] A. Djouadi and G. Moreau, *Phys. Lett. B* **660** (2008) 67 [hep-ph/0707.3800]; N. Maru, *Mod. Phys. Lett. A* **23** (2008) 2737 [hep-ph/0803.0380]; G. Bhattacharyya and T. S. Ray, *Phys. Lett. B* **675** (2009) 222 [hep-ph/0902.1893]; N. Maru, T. Nomura, J. Sato and M. Yamanaka, [hep-ph/0905.4554].
- [8] For recent reviews on technicolor models, see C. T. Hill and E. H. Simmons, *Phys. Rept.* **381** (2003) 235 [hep-ph/0203079]; F. Sannino, hep-ph:0911.0931.
- [9] G. F. Giudice, R. Rattazzi and J. D. Wells, *Nucl. Phys. B* **595** (2001) 250 [hep-ph/0002178].
- [10] C. Csaki, C. Grojean, H. Murayama, L. Pilo and J. Terning, *Phys. Rev. D* **69** (2004) 055006 [hep-ph/0305237]; C. Csaki, C. Grojean, L. Pilo and J. Terning, *Phys. Rev. Lett.* **92** (2004) 101802 [hep-ph/0308038].
- [11] G. Cacciapaglia, C. Csaki, G. Marandella and J. Terning, *JHEP* **0702** (2007) 036 [hep-ph/0611358].
- [12] D. Stancato and J. Terning, *JHEP* **0911** (2009) 101 [hep-ph/0807.3961].
- [13] M. A. Luty and T. Okui, *JHEP* **0609**, 070 (2006) [hep-ph/0409274].
- [14] C. Grojean, [hep-ph/0910.4976]; D. E. Morrissey, T. Plehn and T. M. P. Tait, [hep-ph/0912.3259].
- [15] A. V. Manohar and M. B. Wise, *Phys. Lett. B* **636** (2006) 107 [hep-ph/0601212]; A. Pierce, J. Thaler and L. T. Wang, *JHEP* **0705** (2007) 070 [hep-ph/0609049].
- [16] G. Cacciapaglia, A. Deandrea and J. Llodra-Perez, *JHEP* **0906** (2009) 054 [hep-ph/0901.0927].
- [17] R. Contino, Y. Nomura and A. Pomarol, *Nucl. Phys. B* **671** (2003) 148 [hep-ph/0306259].

- [18] K. Agashe, R. Contino and A. Pomarol, Nucl. Phys. B **719** (2005) 165 [hep-ph/0412089].
- [19] R. Contino, L. Da Rold and A. Pomarol, Phys. Rev. D **75** (2007) 055014 [hep-ph/0612048].
- [20] I. Low, R. Rattazzi and A. Vichi, [hep-ph/0907.5413].
- [21] M. Spira and J. D. Wells, Nucl. Phys. B **523** (1998) 3 [hep-ph/9711410].
- [22] A. Djouadi, J. Kalinowski and M. Spira, Comput. Phys. Commun. **108** (1998) 56 [hep-ph/9704448]. For an update, see A. Djouadi, J. Kalinowski, M. Muhlleitner and M. Spira in J. M. Butterworth *et al.*, [hep-ph/1003.1643].
- [23] P. Bechtle, O. Brein, S. Heinemeyer, G. Weiglein and K. E. Williams, Comput. Phys. Commun. **181** (2010) 138 [hep-ph:0811.4169]. (See also <http://www.ippp.dur.ac.uk/HiggsBounds>)
- [24] R. Barate *et al.* [LEP Working Group for Higgs boson searches], Phys. Lett. B **565** (2003) 61 [hep-ex/0306033]; S. Schael *et al.* [ALEPH and DELPHI and L3 and OPAL Collaborations], Eur. Phys. J. C **47** (2006) 547 [hep-ex/0602042].
- [25] [LEP Higgs Working Group], LHWG Note 2002-02.
- [26] T. Aaltonen *et al.* [CDF and D0 Collaborations], Phys. Rev. Lett. **104** (2010) 061802 [hep-ex/1001.4162];
- [27] The TEVNP Working Group for the CDF and D0 Collaborations, FERMILAB-PUB-09-394-E, CDF Note 9888, D0 Note 5980-CONF.
- [28] M. E. Peskin and T. Takeuchi, Phys. Rev. D **46** (1992) 381.
- [29] R. Barbieri, B. Bellazzini, V. S. Rychkov and A. Varagnolo, Phys. Rev. D **76** (2007) 115008 [hep-ph/0706.0432].
- [30] G. Altarelli and R. Barbieri, Phys. Lett. B **253** (1991) 161.
- [31] M. Spira, Fortsch. Phys. **46**, 203 (1998) [hep-ph/9705337].
- [32] A. Djouadi, Phys. Rept. **457** (2008) 1 [hep-ph/0503172].
- [33] H. M. Georgi, S. L. Glashow, M. E. Machacek and D. V. Nanopoulos, Phys. Rev. Lett. **40**, 692 (1978).
- [34] M. Spira, A. Djouadi, D. Graudenz and P. M. Zerwas, Phys. Lett. B **318** (1993) 347; Nucl. Phys. B **453** (1995) 17 [hep-ph/9504378].
- [35] D. Graudenz, M. Spira and P. M. Zerwas, Phys. Rev. Lett. **70** (1993) 1372. S. Dawson, Nucl. Phys. B **359**, 283 (1991); R. P. Kauffman and W. Schaffer, Phys. Rev. D **49**, 551 (1994) [hep-ph/9305279]; S. Dawson and R. Kauffman, Phys. Rev. D **49**, 2298 (1994) [hep-ph/9310281]; M. Kramer, E. Laenen and M. Spira, Nucl. Phys. B **511**, 523 (1998) [hep-ph/9611272].

- [36] R. V. Harlander and W. B. Kilgore, Phys. Rev. Lett. **88** (2002) 201801 [hep-ph/0201206]; C. Anastasiou and K. Melnikov, Nucl. Phys. B **646**, 220 (2002) [hep-ph/0207004]; V. Ravindran, J. Smith and W. L. van Neerven, Nucl. Phys. B **665** (2003) 325 [hep-ph/0302135].
- [37] S. Catani, D. de Florian, M. Grazzini and P. Nason, JHEP **0307**, 028 (2003) [hep-ph/0306211].
- [38] R. V. Harlander and K. J. Ozeren, Phys. Lett. B **679**, 467 (2009) [hep-ph/0907.2997]; R. V. Harlander and K. J. Ozeren, JHEP **0911**, 088 (2009) [hep-ph/0909.3420]; A. Pak, M. Rogal and M. Steinhauser, Phys. Lett. B **679**, 473 (2009) [hep-ph/0907.2998]; A. Pak, M. Rogal and M. Steinhauser, [hep-ph/0911.4662].
- [39] A. Djouadi and P. Gambino, Phys. Rev. Lett. **73**, 2528 (1994) [hep-ph/9406432]; A. Ghinculov and J. J. van der Bij, Nucl. Phys. B **482**, 59 (1996) [hep-ph/9511414]; A. Djouadi, P. Gambino and B. A. Kniehl, Nucl. Phys. B **523**, 17 (1998) [hep-ph/9712330]; G. Degrossi and F. Maltoni, Phys. Lett. B **600** (2004) 255; [hep-ph/0407249]. U. Aglietti, R. Bonciani, G. Degrossi and A. Vicini, [hep-ph/0610033]; S. Actis, G. Passarino, C. Sturm and S. Uccirati, Phys. Lett. B **670**, 12 (2008) [hep-ph/0809.1301]; C. Anastasiou, R. Boughezal and F. Petriello, JHEP **0904**, 003 (2009) [hep-ph/0811.3458].
- [40] M. Spira, “HIGLU: A Program for the Calculation of the Total Higgs Production Cross Section at Hadron Colliders via Gluon Fusion including QCD Corrections,” [hep-ph/9510347].
- [41] R. N. Cahn and S. Dawson, Phys. Lett. B **136**, 196 (1984) [Erratum-ibid. B **138**, 464 (1984)]; K. I. Hikasa, Phys. Lett. B **164**, 385 (1985) [Erratum-ibid. **195B**, 623 (1987)]; G. Altarelli, B. Mele and F. Pitolli, Nucl. Phys. B **287**, 205 (1987).
- [42] T. Han, G. Valencia and S. Willenbrock, Phys. Rev. Lett. **69**, 3274 (1992) [hep-ph/9206246].
- [43] T. Figy, C. Oleari and D. Zeppenfeld, Phys. Rev. D **68**, 073005 (2003) [hep-ph/0306109]; E. L. Berger and J. M. Campbell, Phys. Rev. D **70**, 073011 (2004) [hep-ph/0403194]; M. Ciccolini, A. Denner and S. Dittmaier, Phys. Rev. D **77**, 013002 (2008) [hep-ph/0710.4749].
- [44] URL: <http://people.web.psi.ch/spira/proglist.html>
- [45] S. L. Glashow, D. V. Nanopoulos and A. Yildiz, Phys. Rev. D **18**, 1724 (1978); Z. Kunszt, Z. Trocsanyi and W. J. Stirling, Phys. Lett. B **271**, 247 (1991).
- [46] T. Han and S. Willenbrock, Phys. Lett. B **273**, 167 (1991).
- [47] O. Brein, A. Djouadi and R. Harlander, Phys. Lett. B **579**, 149 (2004) [hep-ph/0307206].
- [48] M. L. Ciccolini, S. Dittmaier and M. Kramer, Phys. Rev. D **68**, 073003 (2003) [hep-ph/0306234].
- [49] R. Raitio and W. W. Wada, Phys. Rev. D **19**, 941 (1979); J. N. Ng and P. Zakarauskas, Phys. Rev. D **29**, 876 (1984); Z. Kunszt, Nucl. Phys. B **247**, 339 (1984); W. J. Marciano and F. E. Paige, Phys. Rev. Lett. **66**, 2433 (1991).

- [50] W. Beenakker, S. Dittmaier, M. Kramer, B. Plumper, M. Spira and P. M. Zerwas, Phys. Rev. Lett. **87** (2001) 201805 [hep-ph/0107081]; Nucl. Phys. B **653** (2003) 151 [hep-ph/0211352]; S. Dawson, L. H. Orr, L. Reina and D. Wackerroth, Phys. Rev. D **67**, 071503 (2003) [hep-ph/0211438].
- [51] G. L. Bayatian *et al.* [CMS Collaboration], J. Phys. G **34** (2007) 995.
- [52] G. Aad *et al.* [The ATLAS Collaboration], [hep-ex/0901.0512].
- [53] R. K. Ellis, I. Hinchliffe, M. Soldate and J. J. van der Bij, Nucl. Phys. B **297** (1988) 221.
- [54] A. Belyaev, R. Guedes, S. Moretti and R. Santos, [hep-ph/0912.2620].
- [55] M. Pieri *et al.*, [CMS Collaboration], CERN-CMS-NOTE-2006/112.
- [56] E. Accomando *et al.*, [hep-ph/0608079], and references therein.
- [57] V. D. Barger, K. M. Cheung, A. Djouadi, B. A. Kniehl and P. M. Zerwas, Phys. Rev. D **49** (1994) 79 [hep-ph/9306270]. S. Y. Choi, D. J. . Miller, M. M. Muhlleitner and P. M. Zerwas, Phys. Lett. B **553** (2003) 61; [hep-ph/0210077]; C. P. Buszello, I. Fleck, P. Marquard and J. J. van der Bij, Eur. Phys. J. C **32** (2004) 209; [hep-ph/0212396]; R. M. Godbole, D. J. Miller and M. M. Muhlleitner, JHEP **0712** (2007) 031. [0708.0458 [hep-ph]].
- [58] S. Baffioni *et al.*, [CMS Collaboration], J. Phys. G **34** (2007) N23; CMS Note 2006/115.
- [59] S. Abdullin *et al.*, [CMS Collaboration], Acta Phys. Polon. B **38** (2007) 731, CMS Note 2006/122.
- [60] D. Futyan, D. Fortin and D. Giordano, [CMS Collaboration], J. Phys. G **34** (2007) N315, CMS Note 2006/136.
- [61] CMS Collaboration, CMS PAS HIG-08-003.
- [62] M. Dittmar and H. K. Dreiner, Phys. Rev. D **55** (1997) 167 [hep-ph/9608317].
- [63] G. Davatz, M. Dittmar and A. S. Giolo-Nicollerat, [CMS Collaboration], J. Phys. G **33** (2007) N85, CMS Note 2006/047.
- [64] CMS Collaboration, CMS PAS HIG-08-006.
- [65] H. F. Pi, P. Avery, J. Rohlf, C. Tully and S. Kunori, [CMS Collaboration], CMS Note 2006/092.
- [66] D. L. Rainwater, D. Zeppenfeld and K. Hagiwara, Phys. Rev. D **59** (1999) 014037 [hep-ph/9808468]; T. Plehn, D. L. Rainwater and D. Zeppenfeld, Phys. Rev. D **61** (2000) 093005 [hep-ph/9911385].
- [67] D. Cavalli *et al.*, [hep-ph/0203056].
- [68] C. Foudas, A. Nikitenko and M. Takahashi, [CMS Collaboration], CMS Note 2006/088.
- [69] R. D. Cousins, J. T. Linnemann and J. Tucker, Nucl. Instrum. Meth. A **595** (2008) 480.
- [70] Tommaso Dorigo, private communication.